2003

Seam position detection in pulsed gas metal arc welding

Hao Shen
University of Wollongong

Seam Position Detection in Pulsed Gas Metal Arc Welding

by

Hao SHEN

A Thesis Submitted in Fulfillment of the Requirements for the Award of

Master of Computer Science

(Honours)

from
University of Wollongong
School of Information Technology and Computer Science

December 2003

CERTIFICATION

I hereby declare that this submission is my own work, and that, to the best of my knowledge and belief, it contains no material previously published or written by another person, nor material which to a substantial extent has been accepted for the award of any other degree or diploma of a university or other institute of higher learning, except where due acknowledgement is made in the text.

Hao SHEN

Wollongong, December 2003.

TABLE OF CONTENTS

FIGURES

TABLES

NOMENCLATURE

Symbol	Definition	Unit
μ	Mean	
σ	Standard deviation	
ADC	Analog-to-Digital Converter	
AI	Artificial Intelligence	
ANNs	Artificial Neural Networks	
ASP	Analog Signal Processing	
BP	Back-Propagation ANN	
CTWD	Contact Tip-to-Work Distance (Standoff)	mm
DSP	Digital Signal Processing	
DT	Destructive Testing	
EC	Evolutionary Computation	
ESs	Expert Systems	
FFT	Fast Fourier Transform	
FIR	Finite Impulse Response	
FL	Fuzzy Logic	
FT	Fourier Transform	
GMAW	Gas Metal Arc Welding	
HAZ	Heat Affected Zone	
I	Current	Amps
IIR	Infinite Impulse Response	
LOF	Lack of fusion	
LVQ	Learning Vector Quantization	
NDT	Non-Destructive Testing	
P	Power	Watts
PSD	Power Spectral Density	DB/Hz
R	Resistance	Ohms

RSEW	Resistance Seam Welding	
RSW	Resistance Spot Welding	
SOM	Self-Organizing Map	
V	Voltage	Volts
WFS	Wire feed speed	m/min

ABSTRACT

Lack of fusion is a commonly occurring defect in Pulsed Transfer Gas Metal Arc Welding. Under optimum process parameter settings, such defects are mainly caused by positional error of the torch in relation to the joint profile. This project investigated relationships between seam tracking error and welding process parameters in order to detect lack of fusion.

Using digital signal processing techniques, it was found that there existed consistent ***linear*** relationships between torch standoff and process variables in both the time- and frequency-domains. In the time-domain, when the torch standoff increases, the mean values of both current and power decrease, conversely the mean values of voltage and resistance increase. Whilst in the frequency-domain, it was also discovered that the pulse frequency of power supply varies during welding in accordance to changes in the torch standoff linearly. This curious finding was confirmed by the manufacturer as a result of the characteristics of the specific power supply used.

Additionally, when torch oscillation is considered, it was established that torch offset produces distinct patterns in current signal waveforms which is affected by welding setup, such as the joint profile and the oscillation frequency and amplitude of the torch. For girth welding of symmetric joints, the following classification rule was derived in order to successfully monitor weld quality (lack of fusion): *The signature of a 'good' weld has twice the weave frequency. The signature of a 'poor' weld has the same frequency as the weave frequency*. Due to its independent property of the

power supply, this rule enables us to monitor weld quality (detecting lack of fusion) efficiently and robustly for any power supply type.

Finally, several potential solutions for flexible on-line weld quality monitoring were also proposed.

ACKNOWLEDGEMENTS

Firstly I would like to express my sincere appreciation and gratitude to my supervisors, Professor John Fulcher, Professor John Norrish, Doctor Paul Di Pietro, and early in the project to Doctor Leone Dunn, for their helpful assistance, guidance, encouragement and enormous support enabling me to reach completion of my thesis. I would also like to thank them for all the knowledge they endowed on me and for all the time and effort they spent to assist me during this thesis.

Also, I would like to thank Doctor Susan Nulsen and Doctor Friso de Boer, for their time, assistance and advice on the BHP Tin Mill Project. I would also like to thank the technical staff, Mr. Greg Tillman and Mr. Joe Abbott.

Additionally, I would like to thank my examiners, Dr. Rowan Dean and Dr. Domonic Cuiuri, for their valuable suggestions and comments which have been most helpful for improving the quality of this these.

Finally I would like to thank my family and friends for their endless support throughout my course of study.

CHAPTER ONE

INTRODUCTION

1.1 Background

Welding is one of the most important methods of joining metals. It is used in a wide range of industries, from shipbuilding to aircraft manufacturing. Poor quality through weld defects and deviation from designed mechanical properties of welds can result in unsafe products and higher production costs. Consequently, robotic welding was introduced to replace traditional manual welding to realize high productivity and quality improvements, and is now increasingly being employed in real production environments.

The quality of a weld, which is usually unknown during the welding process, can be determined by physical inspection on completion. Quality parameters that may be assessed include weld size, surface appearance, mechanical properties, and type of defects present. The tests are generally categorized into two classes, *Destructive Testing* (DT) and *Non-Destructive Testing* (NDT). Although destructive testing is easy to perform, it is costly because it destroys the structure and integrity of the weld. NDT, such as x-ray, acoustic emission, eddy current and ultrasound, provides a quantified test of weld quality but without destroying the product and thus can reduce costs significantly. Although NDT has been proven effective for weld quality detection, it is difficult to apply in real time [34].

Consequently, on-line quality monitoring of key process signals has evolved in modern welding technology. Weld quality is assessed using the information collected in real time. In other words, during the welding process, weld quality can be established by correlating weld quality parameters to relevant process variables. Such quality estimation can be further used as the basis for determining subsequent corrective actions, such as whether to re-inspect the welds using DT or NDT, repair or scrap the defective weld [28].

Welding can be modelled using partial differential equations. These equations are non-linear. This makes the welding processes difficult to model. Furthermore, the welding process can be highly sensitive to small changes in its setup and process parameters. Even a slight change can result in significant weld quality variation. Therefore the inherent sensitivity of the welding process is generally considered a key barrier in ensuring high weld quality. All these factors make the welding process extremely difficult to model through the use of mathematical modelling.

In recent years, various non-modelling methods and techniques, such as digital signal processing, artificial intelligence, and regression techniques, have been used to model the welding process. Subsequently, on-line monitoring systems have been constructed to ensure consistent, high quality weld [1, 19, 25, 43]. The work presented in this thesis concentrates on the implementation of on-line weld quality monitoring using digital signal processing techniques.

1.2 Motivation and Overview of Research Project

Pulsed Transfer Gas Metal Arc Welding, the process investigated in this research project, is often employed for positional work due to its low heat input characteristic. It offers excellent control of droplet transfer and extends the versatility of spray transfer to lower mean current levels. It has been established that during welding, lack of fusion (LOF) is a commonly occurring defect [36]. Therefore, the development of an on-line monitoring system for LOF is a necessary requirement in real production processes.

Under optimum welding parameter settings (such as torch travel speed and heat input), it has been established that LOF is mainly caused by positional error of the torch in relation to the joint. Therefore, the original motivation of this project was to detect LOF by investigating the relationship between seam tracking error and welding process parameters, from which proper classification rules for weld quality (LOF) could be constructed.

The project consisted of two stages:

1. *Investigation of welding process.* A series of welding trials were designed and undertaken to better understand the welding process and investigate its fundamental underlying characteristics using digital signal processing techniques (viz. statistical and spectral analysis). This work provided the basis for constructing classification rules.

2. *Construction of classification rules*. Based on the findings of stage 1, a classification rule for detecting torch positional error were identified and

constructed. Further trials were also conducted to verify the suitability and robustness of these rules.

1.3 Thesis Objectives

This thesis focuses on obtaining a solution for the on-line detection of welding fusion defects, by monitoring torch positional error. The objectives of the thesis were to:

- review the common technologies applied in weld quality monitoring and control (digital signal processing and artificial intelligence technology);
- investigate the characteristics of the welding process in both the time-domain and the frequency-domain using transient process signals, to provide a basis for building a classification rule.
- construct a classification rule for detecting positional error based on the previous findings.

1.4 Thesis Organisation

This thesis contains six chapters and appendices.

Chapter 1 presents an overview of the project and the thesis scope.

Chapter 2 presents a literature review of welding processes (in particular Gas Metal Arc Welding) and related research methodologies.

Chapter 3 introduces the experimental methods, equipment, and quality assessment techniques used.

Chapter 4 describes the results of the preliminary series of welding experiments, and provides fundamental insights into the process for further classification from statistical and spectral analysis.

Chapter 5 presents the construction and validation of the classification rule for detecting LOF.

Chapter 6 draws the conclusions and suggests further work.

The appendices contain the BHP Tin Mill Project, original analysis results (diagrams) and MATLAB source codes.

CHAPTER TWO

LITERATURE REVIEW

2.1 Welding Process

The work in this thesis focuses on metal processing. Welding is a joining process for metals and nonmetals performed by heating material to a suitable temperature or by application of pressure alone, with or without the use of a filler material. Two or more pieces of metal are brought into contact, to which a welding process is applied that coalesces the materials on an atomic scale. Such union is usually permanent, and makes workpieces behave in the same way as a single piece.

Generally speaking, the welding process can be classified into two categories, *fusion welding* and *nonfusion welding* (also called *welding with pressure*). In fusion welding, the workpieces are heated to above the melting point(s) for a pure material or alloy. Atoms from the materials are brought together in the liquid state to establish material continuity. After solidification, large volumes of primary bonds (welds) are created across the interface.

By contrast, nonfusion welding either employs no heating or only heats the workpieces to below the melting point of the base materials. Through the application of appropriate pressure, the atoms of the materials are squeezed into equilibrium spacing [17].

2.1.1 Resistance Seam Welding

Resistance Seam Welding (RSEW) is commonly classified as a nonfusion welding process, although fusion is always achieved at the interface. During welding, when current flows through the materials, heat is produced from resistance to the current applied. Through the application of additional pressure – usually directly through the electrodes – the heated workpieces are joined together. In resistance seam welding, a series of overlapping spots are produced along the interface of the workpieces (Figure 1), thus RSEW is also regarded as an adaptation of Resistance Spot Welding (RSW) [27]. Copper alloy wheels are commonly selected as electrodes. Such welding techniques are widely employed in making flange welds and watertight joints for tanks.

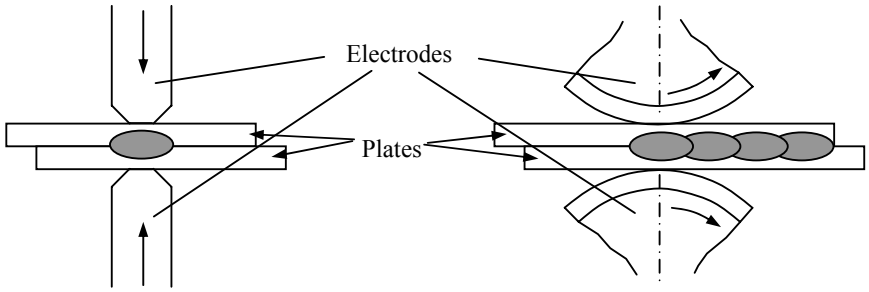

a) Resistance Spot Welding b) Resistance Seam Welding

Figure 1: Resistance Welding.

Initially, this research work was to investigate a RSEW process at BHP's Tin Mill. This investigation was not continued for reasons discussed in Appendix 1.

2.1.2 Gas Metal Arc Welding

Gas Metal Arc Welding (GMAW) is a process in which coalescence is produced by heating with an arc between a continuously fed consumable electrode and workpiece.

It was first introduced in the late 1940s, and has become one of the most popular arc welding processes to date [34].

During welding, droplets of consumable, heated by an arc, travel from the electrode to the workpiece continuously. Simultaneously, shielding gas, provided by an external supply, is used to protect the arc and the weld pool from contamination by the surrounding atmosphere (Figure 2) [7].

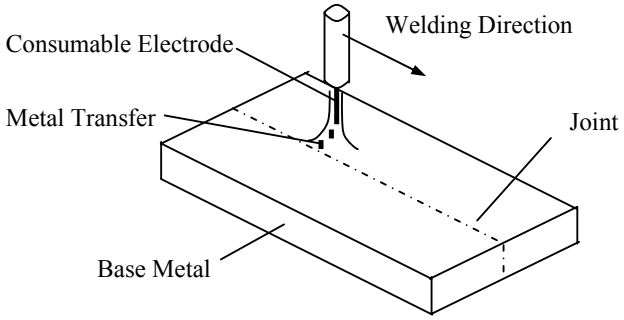

Figure 2: Gas Metal Arc Welding

Robotic GMAW

Conventional GMAW systems, i.e. manually manipulated welding, relies on the welder's sensory perception and experience to ensure adequate weld quality. Obviously, such a welding process is prone to inconsistency.

Robotic welding provides a more reliable technique. Due to the sensitive nature of the process however, inconsistent joint alignment and other variables in the work environment make open-loop robotic welding systems inadequate. Thus seam-tracking technology is an appropriate method to provide feedback control. During welding, selected process variables are sensed by a monitoring system, from which

the control system decides on an action and adjusts the torch position to ultimately ensure consistent weld quality.

Typical sensing techniques include *through-arc sensing*, *spectrum sensing*, *visual sensing,* and *acoustic sensing*. Although each sensing technique has its distinct advantages and disadvantages, through-arc sensing and visual sensing are the most practical solutions employed in real world applications to date.

Through-arc sensing is an easy technique to implement, as it only requires arc voltage and welding current signals. Through-arc sensing can detect arc-start conditions, steady-state arc stability and mode of metal transfer. Furthermore, it can detect the onset of GMAW process disturbances, including variations in torch height, insufficient shielding gas cover, and other variables in the process and conditions [5]. In this project, through-arc sensing was employed for process monitoring.

Girth Welding

GMA Girth welding is a term commonly used for the joining of pipe such as in gas transmission pipelines. Generally, such a process consists of three respective steps, a *root pass*, one or more *fill passes*, and a *final capping pass* (Figure 3). In this project, Pulsed Transfer GMAW was employed to realize fill passes.

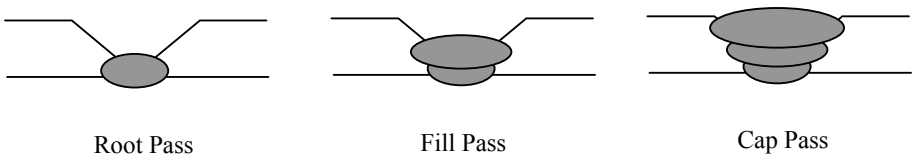

Figure 3: Deposition Runs in Girth Welding.

During GMAW of 'V' butt welds, a common technique used to fill the joint is to oscillate back and forth weaving across the centerline of the groove whilst travelling along the seam. Figure 4 shows the path of the torch along a joint. Such oscillation of the torch results in a change in standoff according to the groove profile.

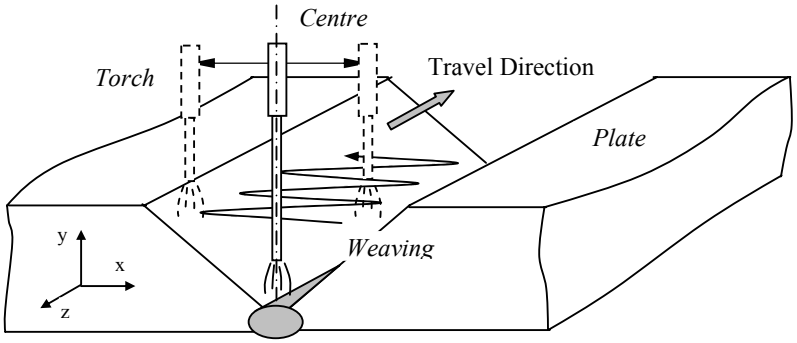

Figure 4: Torch Path in Relation to Joint Seam.

Figure 5 shows a schematic defining several geometric parameters. The *standoff* represents the distance between the contact tip and the workpiece; it is also called the *torch height* or *Contact Tip-to-Work Distance*, *CTWD*. The deviation of the torch centerline from the groove centerline is defined as the *offset* [4].

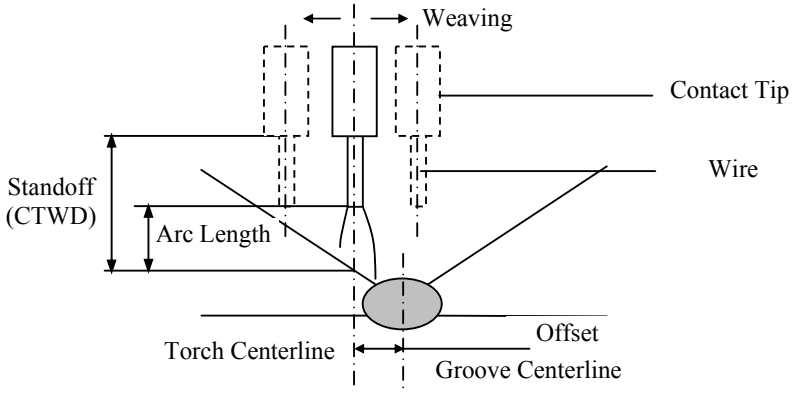

Figure 5: Definition of Geometric Parameters.

Several common defects occur during welding, the category and occurrence rate being listed in Table 1 [36]. Lack of fusion (LOF) – the lack of coalescence between the molten filler metal and the previously deposited filler metal or the sidewall of the joint – is the most commonly occurring defect. It is usually caused by insufficient heat input or poor seam-tracking capability resulting in large torch centerline offset.

Defect	Percentage of Occurrence
Lack of Fusion	66.9%
Porosity	22.0%
Lack of Penetration	4.1%
Burn Through	2.6%
Others	4.4%

Table 1: Defect Occurrence Frequency.

2.2 Research Methodology

2.2.1 Digital Signal Processing

Signals are the description of how one parameter is related to another parameter in an observed system. They generally originate as sensory data from the real world: seismic vibrations, medical images, stock markets, etc. It is very common for information to be encoded in signals. The technique which extracts the information from the signals is called *Signal Processing*. Commonly there are two approaches for analyzing signals, namely the time or frequency domain approaches. In welding applications, the most common types of signals are voltage or current waveforms, which vary with time. Both signals can easily be analyzed by both time and spectral domain methods [38, 40].

Originally, the signals from the real world are *continuous-time* or *analog* in nature. Using an Analog-to-Digital Converter (ADC), the analog signals are sampled and converted to a *digital* form suitable for computer use. Accordingly, signal processing is also categorised into either *Analog Signal Processing* (ASP) or *Digital Signal Processing* (DSP). ASP utilises analog electronic circuits, made up of components such as resistors, capacitors and operational amplifiers, to process the direct analog waveform of the physical quantity. DSP performs numerical calculations on the digitised signals with digital processors, such as PCs, or dedicated Digital Signal Processor chips [18].

In the early 1960s, computers were already being used to explore the possibilities of processing analog signals digitally. Due to the limitation of computer technology at the time however, DSP techniques were hampered. The development of digital computers made it possible for DSP techniques to be used in much wider ranges of applications [47].

Time-domain Analysis

Statistics is a common technique used for analysing time-domain characteristics in DSP. These methods characterize the observed system by describing signals in the form of *mean*, *minimum value*, *maximum value*, and *standard deviation* amongst other attributes [40].

The minimum and maximum values provide information about the range of the signal. The mean (μ) indicates the average value of a signal (Equation 1), whilst the

standard deviation (σ) is a measure of how far the signal fluctuates from the mean (Equation 2).

$$\mu = \frac{1}{N}\sum_{i=1}^{N} x_i \qquad \textit{Equation (1)}$$

$$\sigma^2 = \frac{1}{N-1}\sum_{i=1}^{N} (x_i - \mu)^2 \qquad \textit{Equation (2)}$$

Where N : the number of sampled data points,
x_i : sampled value at data point i.

Frequency-domain Analysis

It has long been established that any continuous signal can be represented as the sum of properly chosen sinusoidal signals. Frequency-domain analysis uses a technique which investigates directly the information encoded in the signal in terms of frequency, phase, and amplitude of the component sinusoids [22].

Fourier Transform (FT) analysis is one of the most important methods in frequency-domain analysis. It calculates a signal's frequency spectrum. With the development of computer technology, especially after the development of the Fast Fourier Transform (FFT) technique by Cooley and Tukey in 1965, the speed of Fourier transform evaluation increased dramatically, which opened up the possibility of using them for real-time control applications in welding.

Another important concept in frequency-domain analysis is frequency filtering. Filters are designed to remove unwanted parts of signals, such as random noise, or to extract useful parts of signals, such as the components lying within a certain frequency range.

According to the filtering algorithm applied, digital filters are generally classified into two types, Finite Impulse Response (FIR) and Infinite Impulse Response (IIR) filters. The FIR filter is known as a non-recursive filter, because the current output is calculated solely from the current and previous input values. By contrast, the IIR filter is a recursive filter, since it uses previous output values in addition to its input values [33].

2.2.2 Artificial Intelligence

Artificial Intelligence (AI) officially commenced in 1956. It attempts to understand, model and implement intelligence systems, such as human intelligence. After several decades of development, various paradigms of AI technology have been developed, with new ones or variations of existing ones being proposed every week. Major AI paradigms include *Expert Systems* (ESs), *Artificial Neural Networks* (ANNs), *Evolutionary Computation* (EC) and *Fuzzy Logic* (FL) [37].

According to their respective characteristics, they are widely used in different areas from financial prediction to engineering simulation [9, 13]. Due to the suitability of AI for modelling complex systems, AI technology was initially investigated as a potential technique for this project.

Expert Systems

Expert Systems focus on specific problem solving. They generally require large amounts of information about a certain domain. The central concept, *knowledge level*,

comprises three components, *goals*, *actions*, and *bodies*, which are usually represented by a well-designed symbolic system.

ESs are comparable to the human reasoning process. They usually require a comprehensive understanding of investigated problems. The greater the information base, the better the ES works. Through manipulations of the knowledge components, the hyperspace of the specific problem is built, and then decisions, such as prediction and classification, can be made.

Although it has been proven that knowledge systems cannot be represented by symbols precisely and completely, easy design and management of an expert system still make it one of the most popular techniques in various specific problem solving areas, such as in game design (e.g. computer chess programs) and finance scheduling.

Artificial Neural Networks

The basic concepts of ANNs were inspired by neuroscience. Biologically, the human brain consists of billions of neurons. Its highly interconnected and parallel structure makes the human brain the most complex and powerful 'computer' in the world. ANNs are parallel computation models, which seek to mimic human brain structure and functions.

The most remarkable feature of ANNs is their adaptive nature, which uses 'learning by example' rather than 'programming'. Problems can be worked out successfully through large amounts of samples, even though the mechanism has not been understood completely. ANNs are very important computational models for a wide

variety of problems, such as those found in pattern classification, associative memory, and noise filtering applications [35].

Evolutionary Computation

Evolutionary Computation, which was founded in the late 1950s, also has a direct root in biological concepts like ANNs. It concentrates on the biological evolutionary process rather than on the structure of biological organs. Natural selection and gene manipulation are two core concepts in EC. Generally, there exist four different paradigms, *Genetic Algorithm*, *Evolutionary Programming*, *Genetic Programming* and *Evolutionary Strategies* [26].

A typical EC model starts with a population of potential solutions for a particular problem. The population of these possible solutions evolves from one generation to another, until a termination condition is reached. Optimization is marked by the most notable characteristic of an EC. Evolutionary computations are also used to construct hybrid techniques with other AI techniques, such as optimal ANN architectures to ameliorate performance [42].

Fuzzy Logic

Fuzzy Logic was developed as a variation of traditional set theory in 1965, by Lotfi Zadeh, Professor of System Theory at the University of California, Berkeley. Conventional logic can explain the substantial world very well. However, it fails in describing human concepts or senses, such as hot or cold and tall or short comparisons. Essentially, FL utilizes a graded statement (probability distribution) rather than a binary statement (strictly *true* or *false*).

Like ES, FL also requires a comprehensive understanding of the working system. It encodes human reasoning steps into a program for making decisions or controlling machinery. Nowadays, FL is most widely used for dynamic systems, especially in engineering control, and for environmental systems.

2.3 DSP and AI Applications in Gas Metal Arc Welding

With the burgeoning of computer techniques over the last several decades, methodologies such as DSP and AI have been widely applied in different welding scenarios, from process simulation and quality monitoring to system control [14, 15, 16, 39].

2.3.1 Control of Arc Length

During arc welding, the arc provides heat which in turn melts the workpiece. When the welding current level is fixed, the distribution and intensity of the heat flux is determined by the length of the arc. In other words, the length of the welding arc determines the distribution of the arc energy, and as a result, the heat input, the width of welds, penetration depth and other quality indices.

Alternatively, if a workpiece is firmly fastened to a welding rig, the length of the welding arc is determined by the torch position (*torch height*, *torch attitude* and *deviation* from the center of the groove). Therefore the measurement and control of torch position play an important role in weld quality monitoring and control [20, 31].

Using DSP techniques, others have shown that torch height variations can be detected by monitoring the change in voltage signal. It has been demonstrated that arc voltage is proportional to the distance of the electrode to the sidewall. Distinct patterns which indicate the symmetrical oscillation of the torch have been observed [8].

Accurate measurements of the torch position and good weld quality have been achieved by constructing control systems based on ANNs [10, 11, 12, 30], with time sequences of process parameters (voltage and current) as inputs. Besides connectionist models, FL controllers have also been successfully developed to keep the arc length constant during welding processes [6].

2.3.2 Control of Weld Pool/Bead

The geometrical characteristic of welds is another essential parameter reflecting weld quality apart from LOF as discussed earlier. It has been demonstrated that the depth of a weld pool determines the mechanical strength of the resulting weld, and that a linear relationship exists between weld penetration and the weld pool width. Therefore, keeping the weld pool size constant is a critical consideration in ensuring consistent weld quality [29].

Spectral analysis has provided evidence that distinct frequency spectra can be related to different pool modes. Based on such findings, ANN and FL classifiers have been successfully constructed to detect the pool mode [2, 12, 45].

Moreover, by constructing an ANN predictor, the depth, width and shape of weld beads can be measured efficiently and precisely (Figure 6). Again, AI technology has demonstrated its strength in applications of GMAW [24].

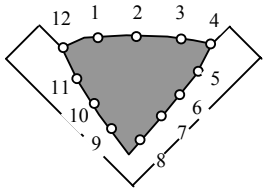

Figure 6: Control of Weld Pool/Bead.

2.3.3 Classification of Metal Transfer Modes

Metal transfer mode is the transfer mechanism by which molten metal travels from the consumable electrode to the workpiece. The mode determines heat input to the weld pool, size and shape of the Heat Affected Zone (HAZ) and weld bead, as well as penetration. Therefore, weld quality can also be estimated and controlled through monitoring of transfer modes. In GMAW systems, there exist three main modes of transfer, *spray mode*, *globular mode* and *short-circuiting mode* [23].

ANN classifiers have been constructed to successfully identify the metal transfer mode. Meanwhile, several ANN paradigms, such as self-organizing maps (SOM), Back-Propagation (BP) and Learning Vector Quantization (LVQ), have also been investigated from the perspective of system performance. Amongst these, SOM offers the best performance in terms of mode classification [41].

2.3.4 Defect Prediction

Apart from estimating weld quality parameters post process, assessing weld defects directly during welding has also been considered recently [21]. Similar methodology has been employed in this project.

By applying statistical methods on the welding signals captured (i.e. histogram distribution of voltage and current), a SOM classifier successfully categorized weld quality into one of three classes, *normal*, *instability*, and *burn through*. However, the classification concentrated on the entire weld seam; in other words, the researchers only investigated whether defects appeared during the weld run rather than the specific location where the defects appeared. For a particular, the SOM classifier therefore had no capacity to specifically locate a weld defect [46].

2.4 Summary

Based on the above review, weld quality parameters (such as arc length, weld pool geometry, and metal transfer modes) are commonly estimated in-process to ensure weld quality. Regardless of the process parameters monitored, the ultimate objective of these studies was to estimate weld quality.

With welding being a complex process, no single feature can be isolated; in other words, these quality parameters, more or less, are interdependent. For instance, arc length determines heat input; metal transfer mode determine weld pool size; and so on. However heat input also affects weld pool size.

The key point for this particular application is whether a unique quality parameter best reflects actual weld quality. As discussed, torch offset error is a key factor in ensuring weld quality. Therefore the work in this project focused on the in-process monitoring of seam-tracking error in GMAW.

CHAPTER THREE

EXPERIMENTAL SYSTEM

3.1 Experimental Setup

A Fronius Transplus Synergic 2700 (Figure 7) is a reliable integrated GMAW power supply, and was selected to provide a controllable and stable electrical output whilst operating in the pulsed transfer mode. A shielding gas (Argoshield Universal 81.25% Ar, 16% CO_2, 2.75% O_2) was employed to protect the weld bead, and the filler wire used was 1.0 mm diameter Bohler NiMo 1 fed at a rate of 5.1 m/min. The welding process parameters used are listed in Table 2.

Figure 7: Fronius Transplus Synergic 2700 Welding Power Supply.

Process	:	Pulsed Transfer GMAW
Filler Wire	:	1.0 mm Bohler NiMo 1- IG AWS A5.28 ER 2.0 90S-G
Parent Material	:	7.1 mm mild steel plate
Shielding Gas	:	Argoshield Universal (81.25% Ar, 16% CO_2, 2.75% O_2) at 20 L/min
Workpiece Preparation	:	API bevel, 60^o included angle, 1.5mm nose, 1.6 mm root gap.
Position	:	1G, Down hand
Equipment	:	Fronius Transplus Synergic 2700
Wire Feed Speed	:	5.1 m/min
CTWD	:	15 mm
Travel Speed	:	250 mm/min
Weave Shape	:	Diagonal
Weave amplitude	:	1.5 Bug-O setting
Weave speed	:	2.5 Bug-O setting
Arc Length	:	+15 units
Dwell	:	0.1 seconds
Measured current (mean)	:	117 Amps
Measured voltage (mean)	:	20.6 Volts
Heat input	:	0.58 KJ/mm

Table 2. Weld Procedure Used

WeldGuard 5000 (Figure 8) was used to collect signals during welding. This is an integrated hardware and software package for monitoring the quality of GMAW, developed by the Cooperative Research Centre for Welded Structures (CRC-WS) at the University of Wollongong, It consists of a desktop computer, a data acquisition card, a signal-conditioning box, sensors, and monitoring software [44].

The sensors detect arc voltage (V), welding current (I), and wire feed speed (WFS), and were connected to the signal-conditioning box. Data from the sensors were sampled at 5000 Hz. Through the data acquisition card, the transient signals were transferred from the signal-conditioning box to the monitoring software. Finally, the sensed data was recorded and saved in binary format (.wgd), ready for further analysis.

Figure 8: Main Panel of Weldguard 5000.

3.2 Data Processing System

3.2.1 Data Preprocessing

All the analysis and computations performed were processed using MATLAB [3, 32], which is a well-known package for DSP. Besides transient voltage and current signals, transient Power (P) and Resistance (R) signals were also evaluated using the following equations.

$$P = V \cdot I; \qquad \textit{Equation (3)}$$

$$R = \frac{V}{I}. \qquad \textit{Equation (4)}$$

An example of sampled transient signals is shown in Figure 9.

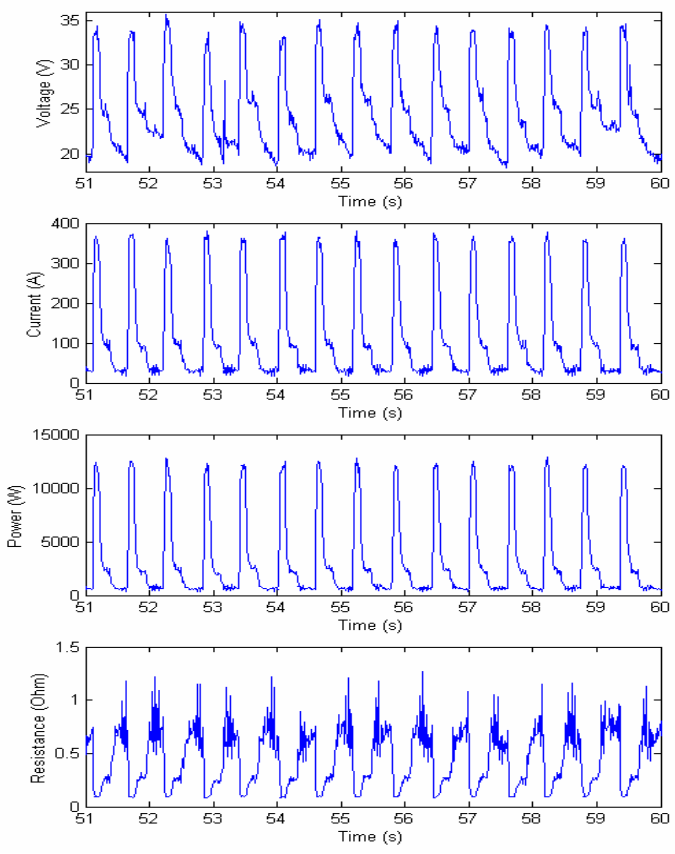

Figure 9: Sample Transient Data (12 sec).

This project investigated signal characteristics in both the time-domain and the frequency-domain. Standard statistical features such as mean, maximum and minimum values were used to monitor average levels and spread. Power Spectral Density (PSD) distribution, resulting from FFT analysis, reflects the frequency component by obtaining the frequency histogram of signals. Figure 10 shows a typical PSD obtained from a captured waveform trace.

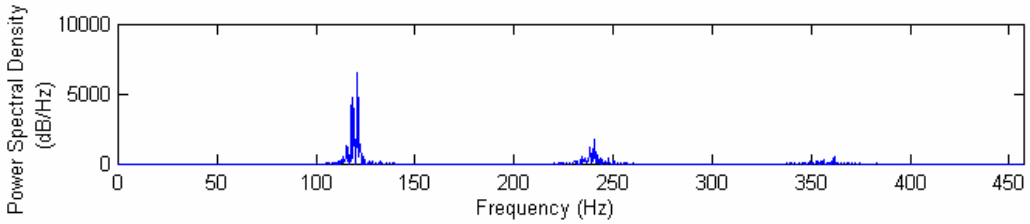

Figure 10: Sample Power Spectral Density Distribution.

It was observed that significant spectral components existed around 120 Hz, 240 Hz and 360 Hz. Clearly the higher frequencies are the second and third harmonics of the lower fundamental component at 120 Hz. Therefore, only the fundamental frequency contents (around 120 Hz) are studied in similar PSD analysis later. Additionally, low frequency components (around 1 Hz) are also considered with special purposes in chapter 5.

The results from the statistical and spectral analysis served as the basis for the classification rules constructed later in this research.

3.2.2 Weld Quality Classification

As disscussed in chapter 1, weld quality is generally established by physical inspection of bead geometry which is normally assessed from the fusion profile of

weld sections. With DT, welds must be sectioned transversely, and then polished and etched. Section profiles can then be inspected and classified as shown in Figure 11.

Generally, weld quality can be assessed on-line in terms of heat input to the weld, the deposition area, and the volume of weld metal deposited per unit time. As a complicated integral system, these criteria are also interrelated. According to the symmetric nature of torch oscillation when the torch is properly aligned above the groove center, equal heat input, fusion, deposited filler metal, and thus equal geometry should exist either side of the joint. In such cases, symmetric weld bead profiles can be expected (Figure 11.a).

When the torch deviates from the groove center, one side of the groove gains greater heat input, more fusion, and more molten filler metal than the other side. Consequently, fusion defects are more likely as one side has too much material deposition whilst the other is lacking. Such welding generally forms non-symmetric weld bead profiles (Figure 11.b).

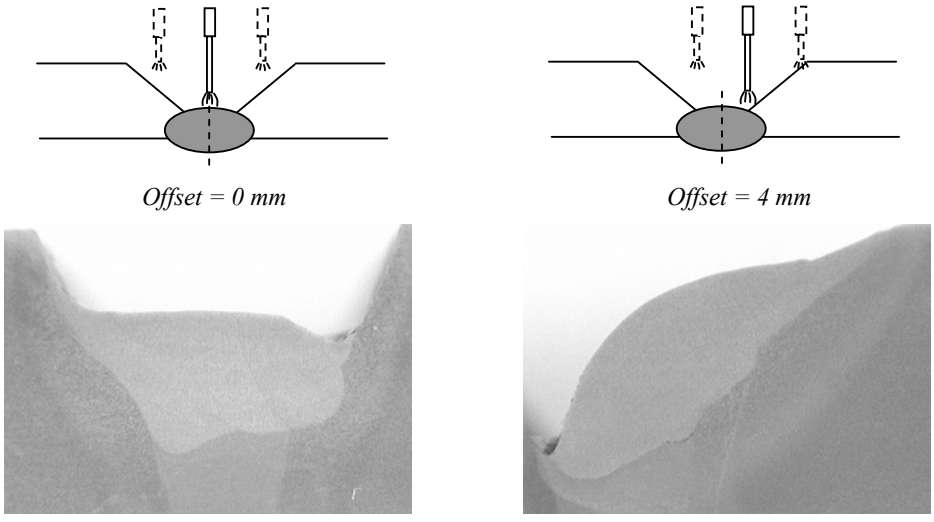

(a) Good Geometry *(b)* Poor Geometry

Figure 11: Torch Offset and Resulting Weld Quality.

Therefore once the correct heat input is established, it can be concluded that a symmetrical weld bead profile indicates 'good' quality, and a non-symmetrical weld refers to 'poor' weld quality. In other words, the larger the offset, the higher the probability of defects appearing. Weld quality is significantly affected by torch position (offset). Therefore the original problem of fusion defect detection has been reduced into a problem of torch position detection or seam-tracking capability.

After inspecting welds of preliminary trials, it was also demonstrated that when using the weld procedure developed, for offsets falling within a certain tolerance (less than 1 mm from the seam centreline approximately), it produced welds classified as acceptable (i.e. 'good' welds). Therefore, in constructing classification rules, robustness of the strategy also needs to be considered.

CHAPTER FOUR

INVESTIGATION OF STANDOFF

Before predicting fusion defects, it is necessary to understand the welding process and its fundamental characteristics in order to aid efficient classification of weld quality. The first consideration is the effect of standoff solely by varying standoff or CTWD (Figure 12). In this series of trials, torch oscillation is not considered.

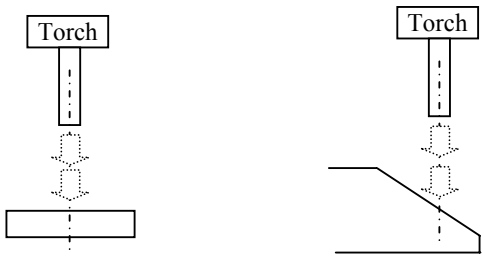

Figure 12: Experiments for Investigating the Effect of CTWD.

4.1 Welding on Flat Plate

For the convenience of adjusting the standoff, the first series of experiments were set up on flat plates (Figure 12.a). Three values of standoff were selected: 10 mm, 15 mm and 20 mm.

Time-domain Analysis

Mean values of process parameters (V, I, P, and R) were calculated and these are listed in Table 3. A consistent trend is evident: when the standoff increases, the mean

values of both I and P decrease. Conversely, the mean values of both V and R increase.

CTWD (mm)	10	15	20
Vmean (V)	23.6525	24.2379	24.5834
Imean (A)	126.6023	109.2405	97.5554
Pmean (kW)	3.4729	3.1440	2.8650
Rmean (W)	0.3718	0.4348	0.4766

Table 3: Mean Values of Process Variables for Flat Plate Trials.

These results indicate that a proportional relationship exists in the time-domain for mean values corresponding to a change in standoff. In other words, there possibly exists a determinate correlation between standoff and the mean values calculated, from which the torch position can be estimated.

Frequency-domain Analysis

Using FFT analysis, a similar, consistent trend in spectral content was also found in the frequency-domain. It was observed that the higher the standoff, the lower the pulse frequency (Figure 13). Additionally, the spectral characteristics of V, P, and R also replicated the same observation as I, and are shown in Appendix 2. Therefore it was established that the findings determined in both the time- and frequency-domains are consistent.

A reasonable conclusion is that when the standoff increases, the frequency content and the means of both current and power decrease; conversely, the frequency components and the mean values of both resistance and voltage increase with an increase in standoff.

This conclusion indicates a consistent correlation between CTWD and the process variable. If such a trend can be verified and identified, it proposes a possible solution for detecting the standoff by simply monitoring the process variables during welding. The next stage of this project was to identify and validate these correlations by increasing the number of welding trials.

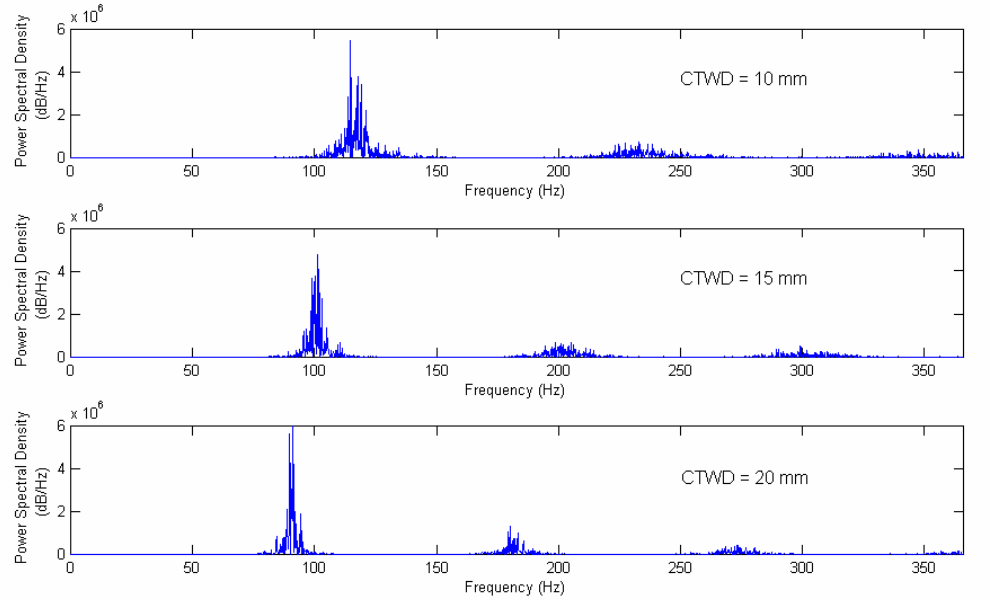

Figure 13: Spectral Analysis of a Current Signal (CTWD = 10, 15, 20 mm).

4.2 Welding on Bevelled plates

A series of experiments, set up on bevelled plates, were designed to verify the findings from the previous trials and to further investigate the effect of directing an arc onto a plane other than at normal incidence (Figure 12.b). In order to identify a more precise relationship between standoff and process variables, the number of standoff variations was increased to 5 (10 mm, 13 mm, 15 mm, 18 mm, and 20 mm).

Time-domain Analysis

Using the same statistical methods employed previously, similar trends were found to those extracted from the flat plate trials (Table 4). It was found that at a standoff of 20 mm, the voltage mean decreased slightly. But this could be due to the greater scatter in results compared to mean current, power and resistance (refer to Figure 14.a). Because the power supply used in this project is a current-based system, it was expected that the current signals should be much more stable than the voltage outputs.

CTWD (mm)	10	13	15	18	20
Vmean (V)	23.8048	23.9885	24.0233	24.3546	24.3319
Imean (A)	148.1098	138.0904	127.8922	113.8908	106.5111
Pmean (kW)	3.9673	3.7419	3.4726	3.1563	3.0025
Rmean (W)	0.3070	0.3419	0.3794	0.4362	0.4574

Table 4: Mean Values of Process Variables for Bevel Trials.

The relationships between torch standoff and the mean values of process parameters were identified as linear, and are shown in Figure 14. Because all the relationships showed similar trends, further experiments only focused on the characteristics of the current signals, as greater analysis of the other attributes seemed superfluous.

Additionally, it was also observed that with some standoffs (10 mm, 15 mm, and 20 mm) as used in the flat plate trials highlighted in Table 4, the current mean values are respectively greater than the results given in Table 3. According to the findings in the previous section (the shorter the arc, the higher the current), this observation can be explained by the angle between the torch and the workpiece surface, which tends to deflect the flexible arc during welding. As illustrated in Figure 15, the actual arc length is generally less than the measured standoff value.

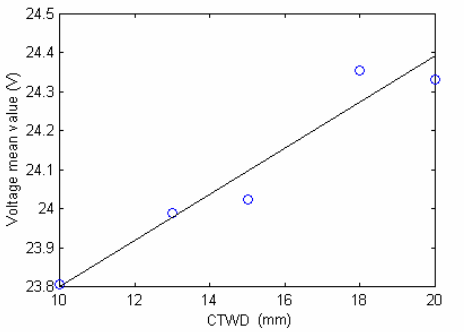

(a) Mean Voltage vs. CTWD;

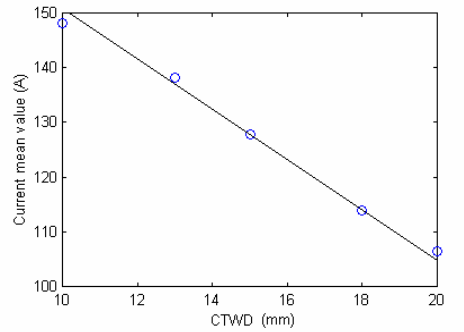

(b) Current Mean vs. CTWD;

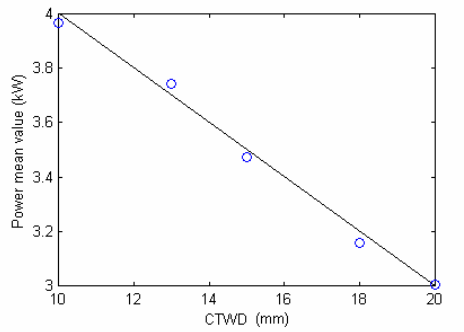

(c) Power Mean vs. CTWD;

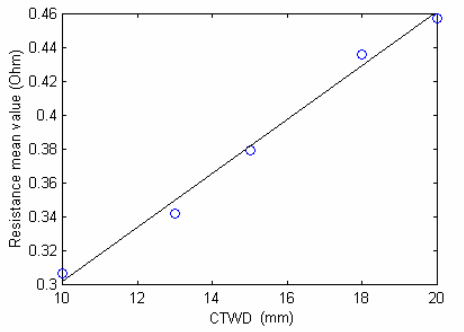

(d) Resistance Mean vs. CTWD;

Figure 14: Relationship between CTWD and Process Variables.

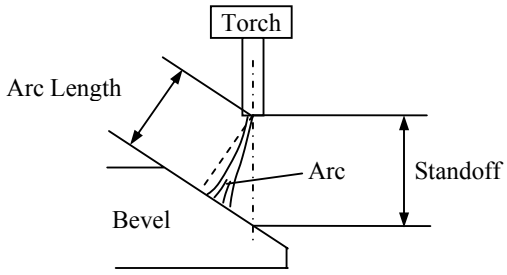

Figure 15: Deflection of Arc.

The above analysis using mean values is a first attempt at characterizing the welding process. A simply transient property commonly investigated in DSP, amplitude, was investigated next. It was expected that a similar observation could also be found in its examination (Figure 16).

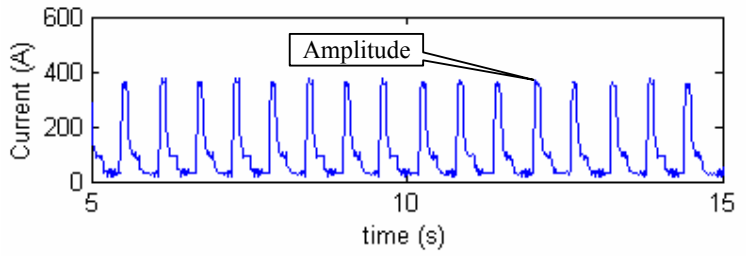

Figure 16: Current Waveform Showing Peak Amplitude.

After extracting the amplitude from the original current signals, an inverse, linearly proportional relationship between standoff and current amplitude was also demonstrated (Figure 17).

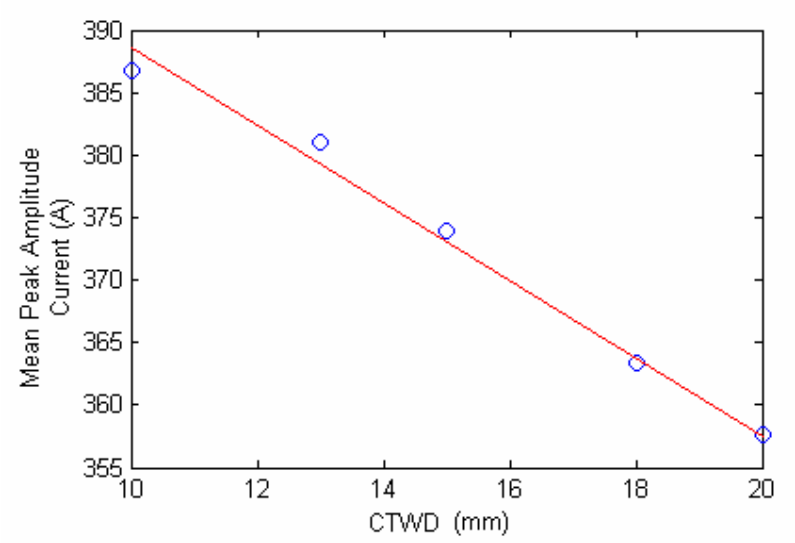

Figure 17: Relationship between CTWD and Mean Peak Amplitude Current.

It was concluded that during the welding process, the change in standoff caused by the torch weaving across the groove would consequently be reflected in a change in amplitude of the transient current signals. It was therefore proposed that a possible solution for detecting torch positional error could be realized by simply monitoring the change in current amplitude on-line.

Frequency-domain Analysis

Based on the PSD analysis (Figure 18), a similar definite shift correlation between standoff and frequency content was also observed in the current signals as in previous trials. It also appears to be linear. However because of the existence of noise and other frequency components, filtering was required to process the signals. The original PSD results for V, P, and R waveforms are presented in Appendix 3.

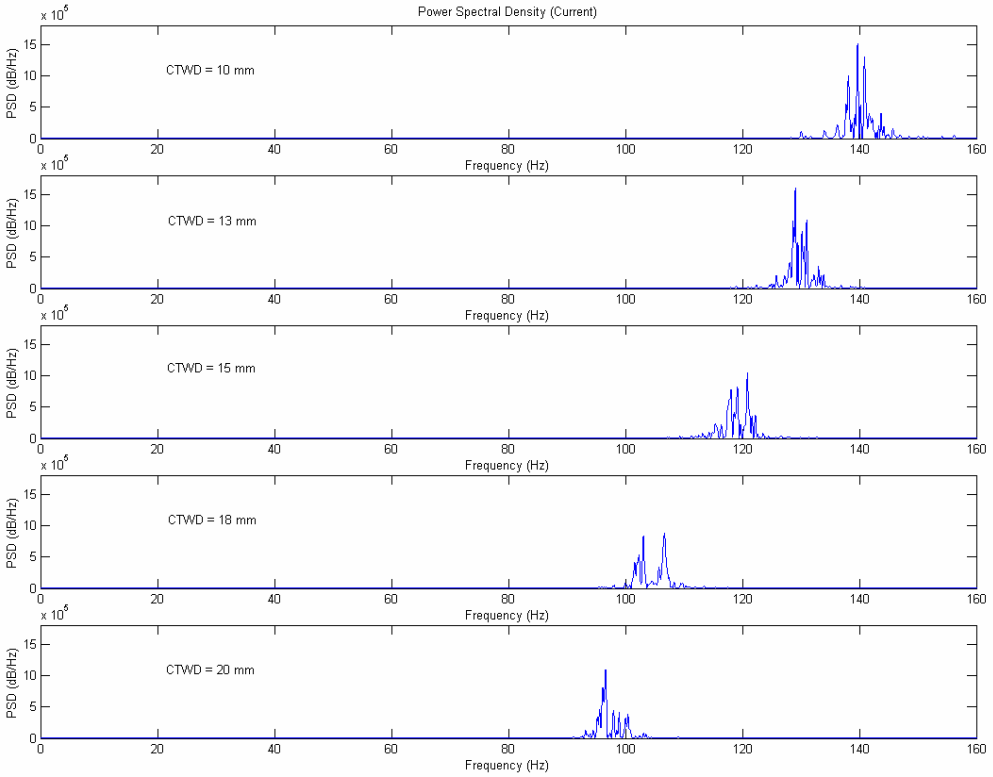

Figure 18: Spectral Analysis of Current Signal
(CTWD = 10, 13, 15, 18, 20 mm)

A Butterworth bandpass filter was therefore applied to extract the dominant frequency. According to the range of the dominant frequencies (100 – 140 Hz approximately), the bandwidth of the filter was set wide enough to ensure that the desired information is retained. Therefore the cutoff frequencies of the bandpass filter were set at 80 Hz and 180 Hz (Figure 19).

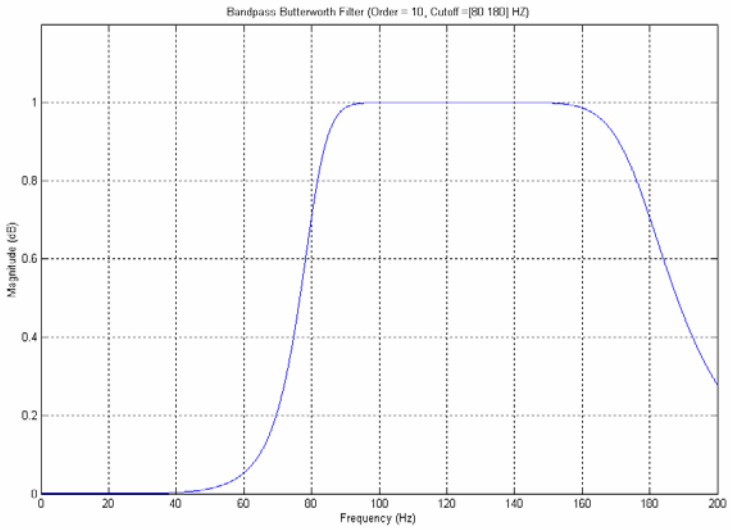

Figure 19: Bandpass Butterworth Filter of Order 10.

Figure 20 shows the original current signals alongside the corresponding filtered results.

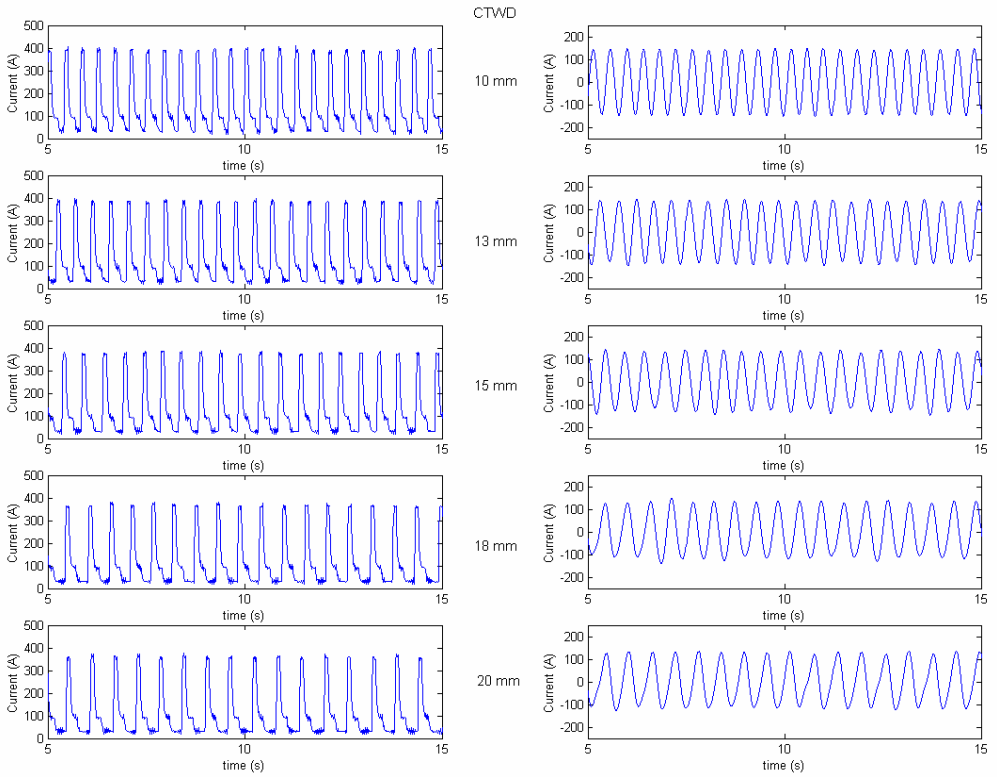

(a) Original Current Signals. *(b)* Filtered Current Signals.

Figure 20: Original and Filtered Current Signals.

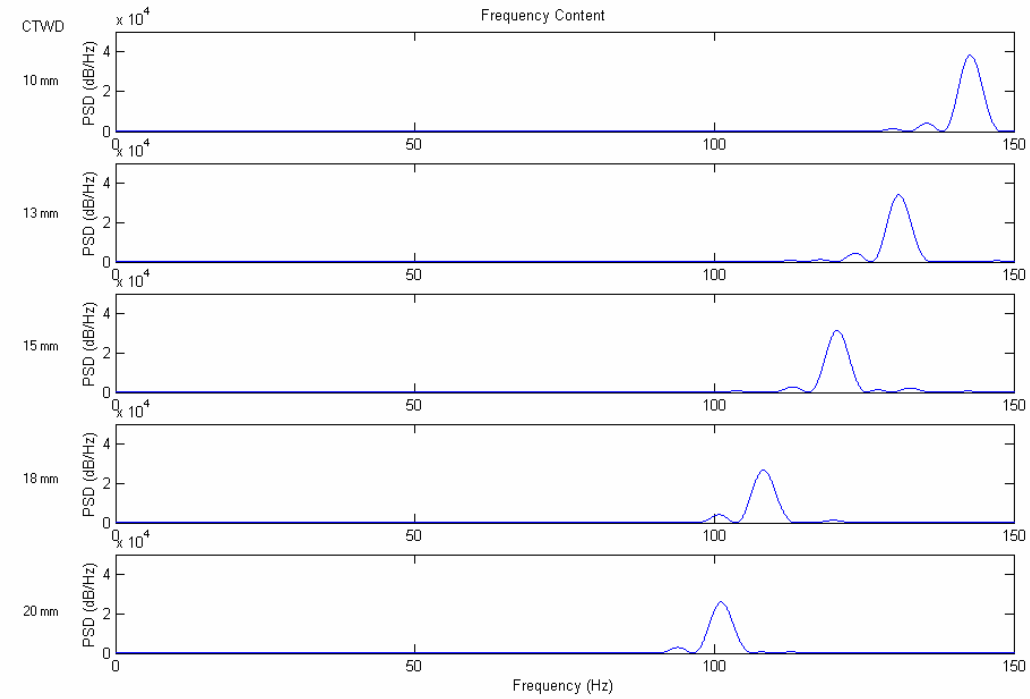

Figure 21: Change of Pulse Frequency.

Conducting spectral analysis on the filtered current signals, the PSD plots appear smoother and it becomes easier to extract peak frequencies (Figure 21). Finally it was confirmed that a linear correlation between standoff and the peak frequency does indeed exist (Figure 22).

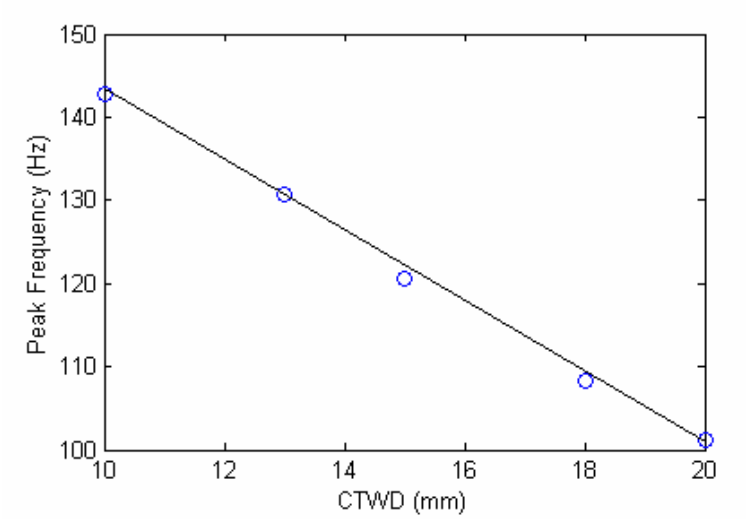

Figure 22: Relationship between CTWD and Peak Frequency.

Therefore it was concluded that under certain power supply settings, torch standoff corresponds to a particular peak frequency, which suggests another option for further classification (i.e. the torch position can be detected via monitoring the change in peak pulse frequency).

Summary:

Based on the investigations undertaken in both the time- and frequency-domains, it was concluded that there exist several *linear* relationships between the torch standoff and the properties of the process signals (both statistical and spectral features). When the torch standoff increases, the peak frequency and the mean values of both current and power decrease. Conversely the mean values of both voltage and resistance also increase.

4.3 Further Study of Pulse Frequency

According to the settings of the power supply, the metal transfer pulse frequency is approximately 120 Hz, which lies exactly in the range of the peak frequencies found (100 – 140 Hz).

Commonly, the pulse frequency of a power source for a given mean current is considered constant during a welding process. From the traces of the original current signals however (Figure 20), it was observed that within a unit time, the number of pulses decreased with an increase in standoff – in other words, the pulse frequency changes during welding in accordance with a change in standoff. A detailed set of signal traces are shown in Figure 23, and the linear relationship is also indicated.

Therefore the peak frequency extracted in the previous section is actually the pulse frequency of the power source. In other words, the pulse frequency of the power supply does indeed change during welding in accordance to changes in the CTWD. This curious finding has been confirmed by the manufacturer (Fronius International GmbH) as a means of accommodating changes in burn off [*Ref*].

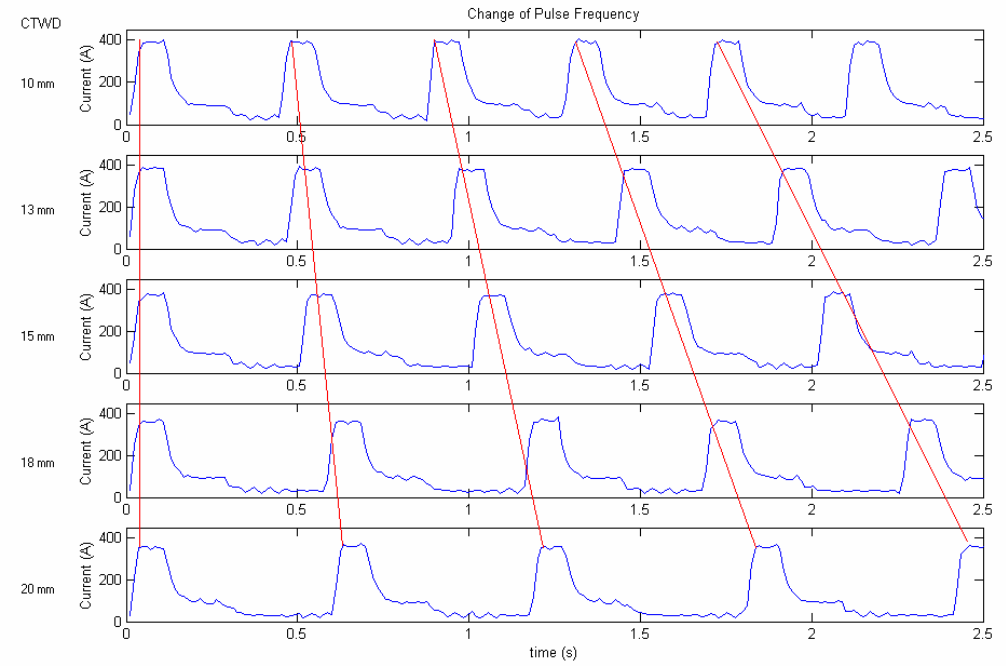

Figure 23: Finer Resolution of Original Current Signals.

[Ref] Private Correspondence, 2003.

CHAPTER FIVE

RULE CONSTRUCTION

5.1 Further Experiments

In this section of work, experiments were designed to investigate the characteristics of the process whilst oscillating the torch during welding. The torch offset-to-joint centerline was set at three different values (0 mm, 2 mm, and 4 mm).

Figure 24 illustrates the characteristics (distinct patterns) of CTWD values varying with time during welding. Because both the joint profile and the oscillation frequency and amplitude of the torch are known, a certain torch offset corresponds to a distinct pattern in the CTWD waveform. In other words, torch offset can be monitored by examining the distinct pattern in changing CTWD.

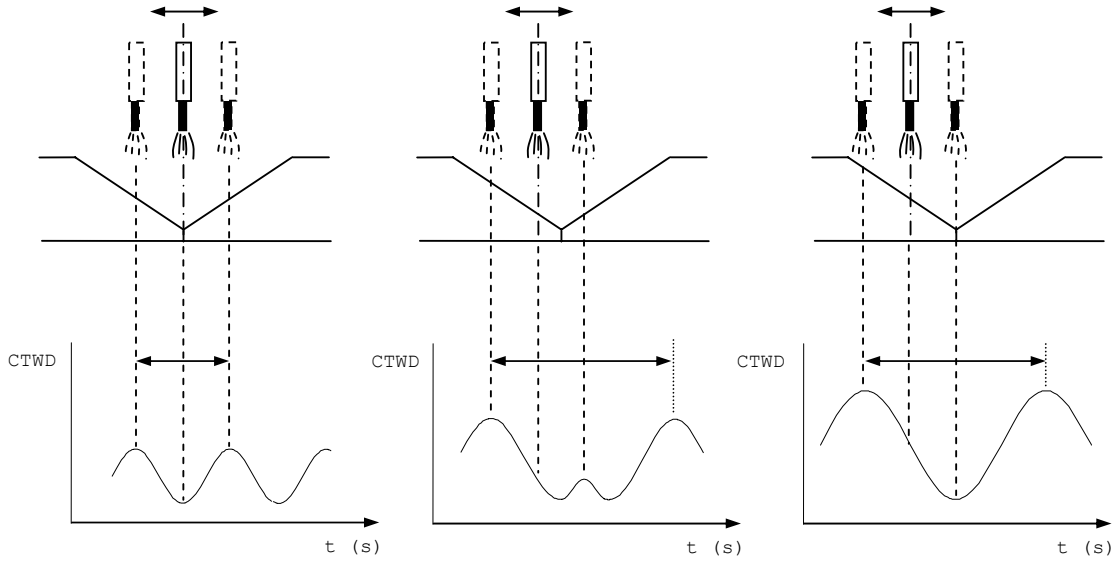

(a) No offset; *(b)* Slight offset; *(c)* Large offset;

Figure 24: Effect of Torch Offset on CTWD.

Furthermore during welding, according to the symmetric nature of torch oscillation, the torch will reach a certain furthermost position, thus the CTWD will reach a certain value on either side of the joint. Additionally, because the joint processed in this project is also symmetrical, when the torch is aligned directly above the groove center (offset = 0 mm), the torch will reach equally either side of the joint (refer to Figure 24.a). Therefore it was predicted that the oscillation frequency of welding with a torch offset would be half of the frequency of welding correctly on the seam centreline.

According to the findings in the previous chapter (i.e. the consistent linear relationships between CTWD and process parameters), the distinct CTWD patterns will be consequentially transferred into the current signal waveforms. Due to the periodic nature of torch oscillation, the torch weaving frequency should also be reflected in the current signals. Therefore the work of the next stage was to investigate the existence of the torch oscillation frequency in the current waveforms.

5.2 Rule Construction

For verifying the existence of torch oscillation frequency, a FFT analysis was performed on a sample current signal. It was found that, in addition to the high frequency components (pulse frequency around 120 Hz), there also existed a much weaker, low frequency content around 1 Hz (Figure 25). According to the welding system settings, the torch oscillation frequency was set at around 1 Hz. Thus the torch oscillation frequency is reflected in the transient current signals.

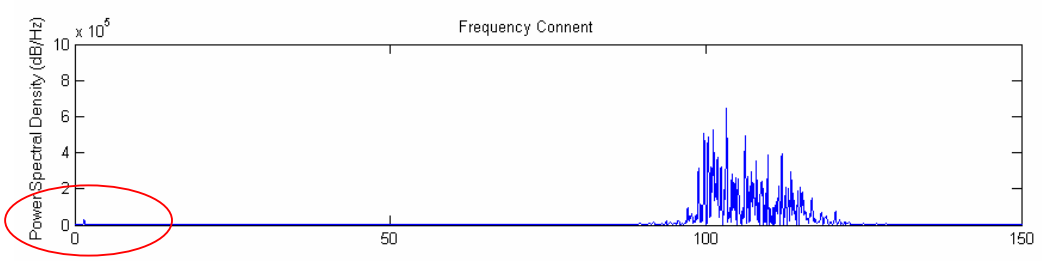

Figure 25: Low Frequency Contents (Weave Frequency) Highlighted in a Current PSD.

A Lowpass Butterworth filter was consequently applied to extract the desired low frequency contents from the original signals. Since the range of expected frequency was less than 2 Hz, the cutoff frequency of the filter was set at 6 Hz (Figure 26), which gave a sufficiently large bandwidth to extract the low frequency information.

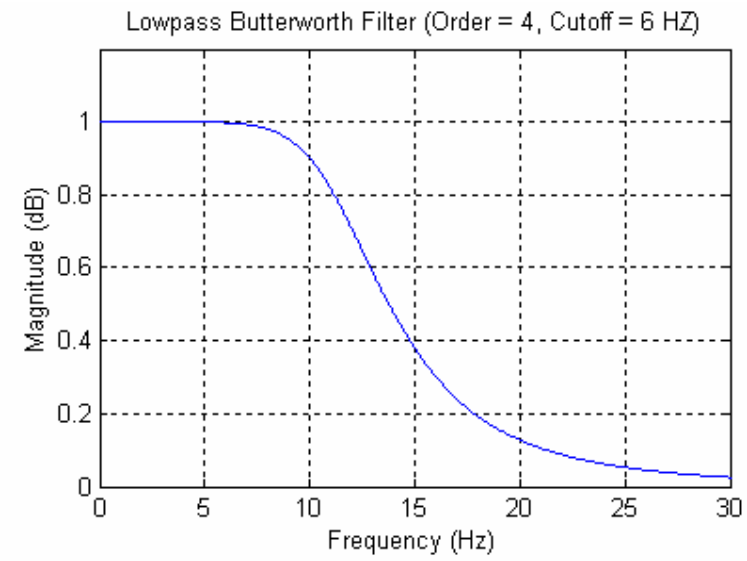

Figure 26: Lowpass Butterworth Filter of Order 4.

Figure 27 shows the filtered signals and the PSD of the corresponding signals. The filtered current waveforms (Figure 27.a) demonstrate similar distinct patterns as those proposed in Figure 24.

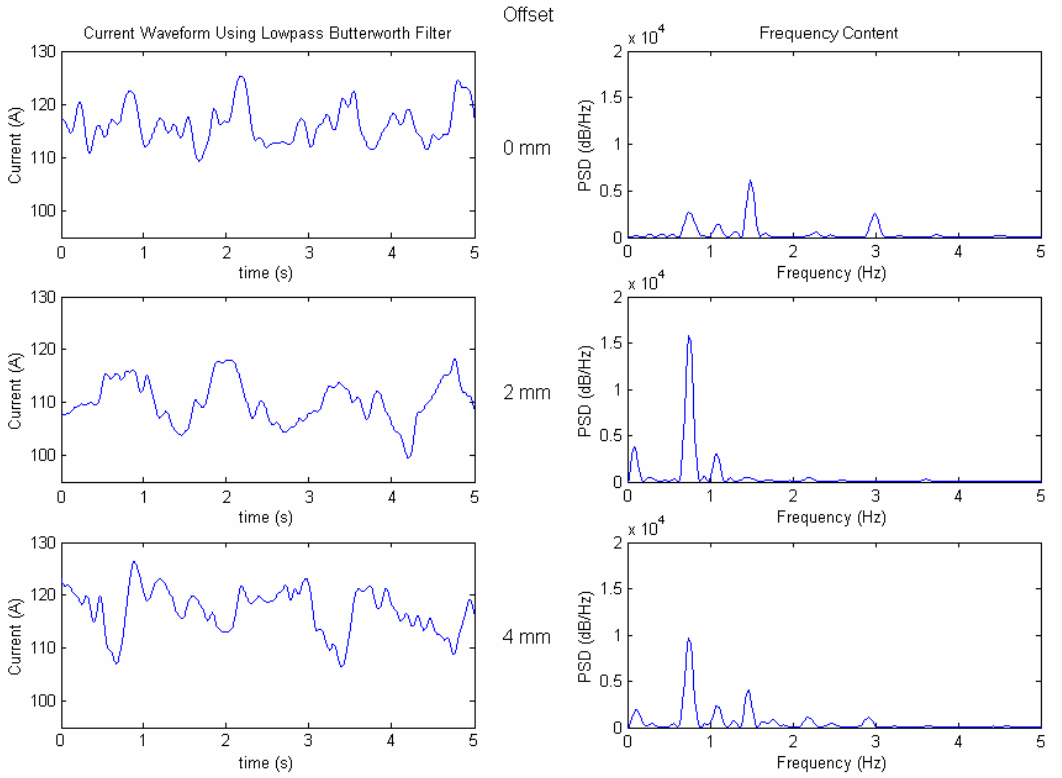

(a) Filtered Signals; *(b)* PSD of Filtered Signals;

Figure 27: Results after Filtering and Corresponding Frequency Contents.

Based on the PSD analysis (Figure 27.b), it was observed that the peak frequency, which indicates the frequency of torch weaving, of symmetrical welding (offset = 0 mm) is twice the frequency of offset welding (offset = 2, 4 mm). These results are summarized in Table 5.

Furthermore, physical inspection of the welds demonstrated that the weld quality with zero offset was assessed as 'good', whilst the other two welds were identified as 'poor' (refer to Figure 11). As presented in chapter 3, 'good' refers to a symmetrical weld profile and 'poor' refers to a non-symmetrical weld.

Offset (mm)	*Weld Quality*	*Frequency (Hz)*
0	Good	1.5259
2	Poor	0.7629
4	Poor	0.7629

Table 5: Frequency Correlation to Offset and Quality.

Therefore a simple but clear classification rule can be constructed:

> ***The signature of a 'good' weld has twice the weave frequency. The signature of a 'poor' weld has the same frequency as the weave frequency.***

5.3 Validation

In order to verify the efficiency of the classification rule, a 'diagonal' weld run was designed and performed. During welding, the torch traveled from the edge of the bevel to the centre of the groove; the offset value changing from 2 mm to 0 mm (Figure 28). According to the classification rule, it was expected that the halving relationship of oscillation frequency would be identified and confirm to the results presented in the previous section.

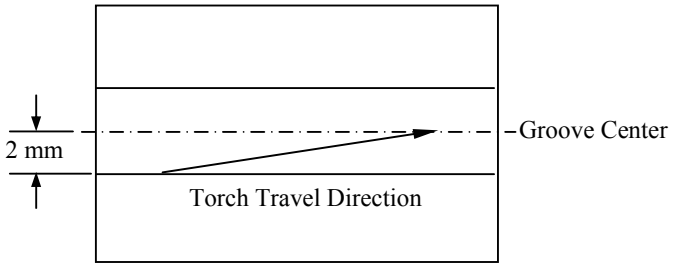

Figure 28: Verifying Experiment.

After signal processing with the same Lowpass Butterworth Filter (refer to Figure 26), the processed current signal was split into three sequential segments (windows), all of

which contain the same number of data points (Figure 29). The PSD results show the oscillation frequency in the first segment (starting at the edge of the bevel) was 0.6866 Hz, whilst the frequency of the third section (finishing on the seam centreline) was 1.3733 Hz.

Edge

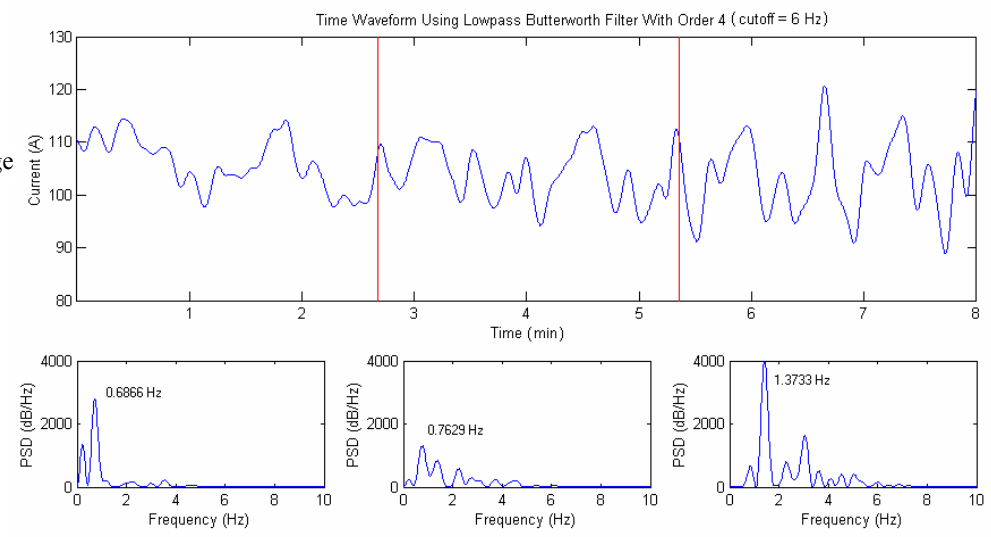

Center

Figure 29: Change of Oscillation Frequency.

Furthermore, it was also demonstrated that the portion of the weld in the third section, where the torch offsets are less than ⅔ mm, were all categorized as 'good'. This confirms the earlier tolerance requirement for classification robustness of 1 mm for 'good' welds.

These results indicate that the constructed classification rule is appropriate for detecting torch positional error during welding, and thus defect detection on-line.

CHAPTER SIX

CONCLUSIONS AND FURTHER WORK

6.1 Conclusions

Using the particular experimental system available for this project without weaving, it was established that during pulsed GMAW, there existed several ***linear*** relationships between torch standoff and properties of process variables in both the time- and frequency-domains. In the time-domain, when the torch standoff increases, the mean values of both current and power decrease, conversely the mean values of both voltage and resistance increase. Whilst in the frequency-domain, it was also discovered that the pulse frequency of the power supply varies during welding in accordance to changes in the torch standoff linearly. This curious finding was confirmed by the manufacturer as a result of the characteristics of the specific power supply used.

Based on the fact that the CTWD patterns vary with time during weaving, it was demonstrated that a distinct torch offset corresponds to a unique CTWD waveform, which depend on the welding setup used, such as the joint profile and the oscillation frequency and amplitude of the torch. Due to the linear correlation between CTWD and the properties of process variables, it was consequentially established that the torch offset position could be monitored by simply examining the distinct patterns in current waveforms.

Furthermore, in the case of symmetrical joint profiles commonly used in pipeline construction, a classification rule was constructed and validated according to the distinct patterns, namely: *The signature of a 'good' weld has twice the weave frequency. The signature of a 'poor' weld has the same frequency as the weave frequency*. As this rule is independent of the power supply used, it enables monitoring of weld quality (detecting LOF) efficiently and robustly regardless of power supply type.

6.2 Recommendations for Further Work

This project has demonstrated that consistent linear correlations exist between CTWD and key process attributes in both the time- and frequency-domains. This in turn could lead to possible solutions for the development of flexible on-line monitoring and control systems for ensuring high quality welds. The following work could further enhance the usefulness of these findings.

1. For welding processes without torch oscillation, according to the linear correlations discovered in both the time- and frequency-domains, on-line control systems for torch height regulation could be developed to ensure weld quality by simply monitoring mean values of process variables, mean peak amplitude current, or pulsed metal transfer frequency signals using basic statistical techniques.

2. For welding processes with torch oscillation, because of the distinct low frequency CTWD patterns generated in accordance with the joint profile,

further work could focus on the development of an intelligent system. This system could dynamically scan the transient signal patterns on-line (e.g. ESs or ANNs), to detect torch misalignment (offset). If the joint is symmetrical as was investigated experimentally, monitoring and control systems based on the constructed classification rule could also be implemented.

3. Furthermore, besides applications monitoring torch height, when torch oscillation is considered, the linear correlation between torch height and pulse frequency could also be applied on-line to detect torch offset on-line to ensure high quality welds. By monitoring changes in pulse frequency and using time-varying pattern detection techniques, this strategy is possible in real-time.

Generally, the findings in both the time- and frequency-domains would be feasible for developing real-time torch height control systems or in-process seam tracking control systems. However, while spectral properties can be extracted efficiently using FFTs in real time, due to the simplicity of statistical techniques, further work is needed to establish the most effective method for on-line real-time closed loop control to avoid defect occurrence.

REFERENCES:

[1] Adolfsson, S., Bahrami, A., Bolmsjo, G. and Claesson I. (1999). *On-Line Quality Monitoring in Short-Circuit Gas Metal Arc Welding*. Welding Research Supplement of Welding Journal, Pg. 59 – 73.

[2] Alzamora, G., Ikeya, H., Kaneko, Y., Ohshima, K., and Chen, Q. (1992). *Intelligent Welding Robot System*. Proceeding of Singapore International Conference on Intelligent Control and Instrumentation. 17 – 21 February 1992. Vol. 2, Pg. 1058 – 1062.

[3] Ambardar, A. and Borghesani, C. (1998). *Mastering DSP concepts using MATLAB*. Prentice Hall.

[4] Bae, K.-Y., Lee, T.-H. and Ahn, K.-C. (2002). *An Optical Sensing System for Seam Tracking and Weld Pool Control in Gas Metal Arc Welding of Steel Pipe*. Journal of Materials Processing Technology, No. 120. Pg 458 – 465.

[5] Barborak, D., Conrardy, C., Madigan, B. and Paskell, T. (1999). *"Through-Arc" Process Monitoring Techniques for Control of Automated Gas Metal Arc Welding*. Proceeding of 1999 IEEE International Conference on Robotics & Automation, Detroit, Michigan. 10 – 15 May 1999. Pg 3053 – 3058.

[6] Bingul, Z., Cook, G.E. and Strauss, A.M. (2000). *Application of fuzzy logic to spatial thermal control in fusion welding*. IEEE Transactions on Industry Applications. Vol. 36. Issue. 6. Nov/Dec. Pg. 1523 – 1530.

[7] Cary, H. B. (1979). *Modern Welding Technology*. Prentice-Hall.

[8] Corlett, B. J., Lucas, J. and Smith, J. S. (1991). *Sensors for narrow-gap welding*. Science, Measurement and Technology, IEE Proceedings-A, Vol. 138. No. 4. Pg. 1409 – 1414.

[9] Eberhart, R. C., Dobbins, R. W., and Simpson, P. K. (1996). *Computational Intelligence PC Tools*. Academic Press Professional, Inc.

[10] Eguchi, K., Yamane, S., Horinaka, S., Kubota, T. and Oshima, K. (1997). *Sensing of groove gap and torch position using neural network in pulsed MIG welding*. IEEE Industrial Electronics, Control and Instrumentation. Vol. 3. Pg. 1409 – 1414.

[11] Eguchi, K., Yamane, S., Sugi, H., Kubota, T. and Oshima, K. (1998). *Application of neural network to detection of arc length, extension length and root gap in robotic welding*. Proceedings of the 24th Annual Conference of the IEEE. Aachen, Germany. 31 Aug – 4 Sep 1998. Vol. 2. Pg. 1131 – 1135.

[12] Hartman, D. A., DeLapp, D. R., Cook, G. E. and Batnett, R. J. (1999). *Intelligent fusion control throughout varying thermal regions*. Proceeding of IEEE Industry Applications Conference. Phoenix, AZ, USA. 3 – 7 Oct 1999. Vol. 1. Pg. 635 – 644.

[13] Hoffmann, A. (1998). *Paradigms of Artificial Intelligence: A Methodological and Computational Analysis.* Springer-Verlag Ltd.

[14] Ivezic, N., Allen, J.D. jr. and Zacharia, T. (1999). *Neural Network-Based Resistance Spot Welding Control and Quality Prediction.* Proceedings of the Second International Conference on Intelligent Manufacturing and Processing of Materials (IPMM '99), Honolulu, 10 – 15 Jul 1999. Vol. 2. Pg 989-994.

[15] Kang, S. I., Kim, G. H., and Lee, S. B. (1999). *A study on the horizontal fillet welding using neural networks*. Proceedings of Third International Conference Knowledge-Based Intelligent Information Engineering Systems. Adelaide, SA, Australia. 31 Aug – 01 Sep 1999. Pg. 217 – 221.

[16] Kim, G. H., Kang, S. I. And Lee, S. B. (1999). *A study on the estimate of weld bead shape and the compensation of welding parameters by considering weld defects in horizontal fillet welding*. Proceedings of Third International Conference Knowledge-Based Intelligent Information Engineering Systems. Adelaide, SA, Australia. 31 Aug – 01 Sep 1999. Pg. 212 – 216.

[17] Jeffus, L. F. (1992). *Welding: principles and applications*. Delmar Publishers, Inc, 3rd edition.

[18] Jones, N. B. and Watson, J. D. Mck. (1979). *Digital signal processing: principles, devices and applications*. Peregrinus Ltd.

[19] Lee, S., Choo, Y., Lee, T., Han, C. and Kim, M. (2000). *Neuro-Fuzzy Algorithm for Quality Assurance of Resistance Spot Welding.* Proceedings of IEEE Industry Applications Conference. Rome, Italy. 08 – 12 Oct 2000. Vol. 2. Pg 1210 – 1216.

[20] Li, P. and Zhang, Y. M. (2001). *Robust sensing of arc length*. IEEE Instrumentation and Measurement. Vol. 50. Issue. 3. Pg. 697 – 704.

[21] Li, D., Song and Ye F. (2000). *On Line Monitoring of Weld Defects for short-circuit Gas Metal Arc Welding Based on the self-Organize Feature Map Neural Networks*, IEEE Transactions on Neural Networks. Vol. 5. Pg. 239 – 244.

[22] Lynn, P. A. and Fuerst, W. (1994). *Introductory digital signal processing with computer applications*. J. Wiley & Sons, Revised edition.

[23] Messler, R. W. Jr. (1999). *Principles of Welding: Processes, Physics, Chemistry, and Metallurgy*. Wiley-Interscience.

[24] Moon, H. S., and Na, S. J. (1997). *Optimum Design Based on Mathematical Model and Neural Network to Predict Weld Parameters for Fillet Joints*. Journal of Manufacturing Systems. Vol. 16. No. 1. Pg. 13 – 23.

[25] Nayak, N. and Ray, A. (1993). *Intelligent seam tracking for robotic welding*. Springer-Verlag Ltd.

[26] Nilsson, N. j. (1998). *Artificial intelligence: A New Synthesis.* Morgan Kaufmann Publishers, Inc.

[27] Norrish, J. (1992). *Advanced Welding Process*. New Manufacturing Processes and Materials Series. Institute of Physics Philadelphia.

[28] Ogunbiyi, T. E. B. (1995). *Process monitoring and adaptive quality control for robotic gas metal arc welding*. Doctor of Philosophy of Engineering Thesis, School of Industrial and Manufacturing Science, Cranfield University.

[29] Ohshima, K., Hirai, A. and Yamane, S. (1995). *Knowledge based information processing of the weld pool using neural network in the robotic welding*. Proceedings of International IEEE/IAS Conference on Industrial Automation and Control: Emerging Technologies. Taipei, Taiwan. 22 – 27 May 1995. Pg. 47 – 51.

[30] Ohshima, K., Yabe, M., Akita, K. and Kugai, K. (1995). *Sensor Fusion Using Neural Network in the Robotic Welding.* Proceedings of IEEE Industry

Applications Conference. Orlando, FL, USA. 8 – 12 Oct 1995. Vol. 2. Pg. 1764 – 1769.

[31] Ohshima, K., Yamane, S., Yabe, M., Akita, K., Kugai, K. and Kubota, T. (1995). *Controlling of Torch Attitude and Seam Tracking Using Neuro Arc Sensor*. Proceedings of the 1995 IEEE IECON 21st International Conference on Industrial Electronics, Control, and Instrumentation. Orlando, FL, USA. 6 – 10 Nov 1995. Vol. 2. Pg. 1185 – 1189.

[32] Ozcelik, S. (1998). *An Animated MATLAB/SIMULINK Tool for Gas Metal Arc Welding Control Experimentation*. Proceedings of the 1998 American Control Conference. Philadelphia, PA, USA. 21 – 26 Jun 1998. Vol. 3. Pg. 1767 – 1771.

[33] Parks, T.W. and Burrus, C.S. (1987). *Digital filter design*. Wiley.

[34] Patton, W. J. (1967). *The Science and Practice of Welding*. Prentice-Hall, Inc.

[35] Pham, D. T. and Liu, X. (1995). *Neural Networks for Identification, Prediction, and Control*. Springer-Verlag Ltd.

[36] Purdevski, M. (2000). *Defect Detection of Automated Gas Metal Arc Pipe Welding*. Master of Engineering Thesis. Department of Mechanical Engineering. University of Wollongong.

[37] Russell, S. J. and Norvig, P. (1995). *Artificial intelligence: A Modern Approach.* Prentice-Hall, Inc.

[38] Schwartz, M. and Shaw, L. (1975). *Signal processing: discrete spectral analysis, detection, and estimation*. McGraw-Hill.

[39] Smith, J. S., (2002). *Artificial Intelligence*. WTIA/TWI/UOW Computer Workshop, 50th WTIA Annual Conference and the 12th International TWI

Computer Technology in Welding and Manufacturing Conference. Wollongong, Australia. 26, August, 2002.

[40] Smith, S. W. (1999). *The Scientist and Engineer's Guide to Digital Signal Processing.* California Technical Publishing. Second Edition.

[41] Vincent, D., McCardle, J. and Stroud, R. (1995), *Classification of Metal Transfer Mode Using Neural Networks*. Proceedings of IEEE International Conference on Neural Networks. Perth, WA, Australia. 27 Nov – 01 Dec 1995. Vol. 1. Pg. 522-525.

[42] Vonk, E., Jain, L. C. and Johnson, R. P. (1997). *Automatic Generation of Neural Network Architecture Using Evolutionary Computation*. Proceedings of Electronic Technology Directions to the Year 2000. Adelaide, SA, Australia. 23 – 25 May 1995. Pg. 144 – 149.

[43] Wei, E., Farson, D., Richardson, R. and Ludewig, H. (2001). *Detection of Weld Surface Porosity by Statistical Analysis of Arc Current in Gas Metal Arc Welding.* Journal of Manufacturing Processing. Vol. 3. No. 1. Pg. 50-59.

[44] *WeldGuard – Advanced Monitoring System for Gas Metal Arc Welding*. User Manual Version 2.2. Cooperative Research Centre for Welded Structures, University of Wollongong. (1998).

[45] Yamane, S., Kaneko, Y., Kitahara, N., Ohshima, K. and Yamamoto, M. (1993). *Neural network and fuzzy control of weld pool with welding robot*. Conference Record of the 1993 IEEE Industry Applications Society Annual Meeting. Toronto, Ont., Canada. 2 – 8 Oct 1993. Vol. 3. Pg. 2175 – 2180.

[46] Ye, F., Song Y. L., Li, D. and Rehfeldt, D. (2002). *Penetration evaluation in robotized arc welding based on support vector machines.* International Institute of Welding, Doc. 212 – 1020 – 02.

[47] Yuen, C. K. and Fraser, D. (1979). *Digital Spectral Analysis*. Pitman Publishing Limited.

APPENDIX 1: The BHP Tin Mill Project

At BHP's Tin Mill, RSEW process was conducted to join two steel coils together (Figure 30). Because welding failures are costly and unsafe, the company was seeking to find an appropriate method to decrease the failure rate. The original motivation of this project was to increase the weld failure detection rate using artificial intelligence technique.

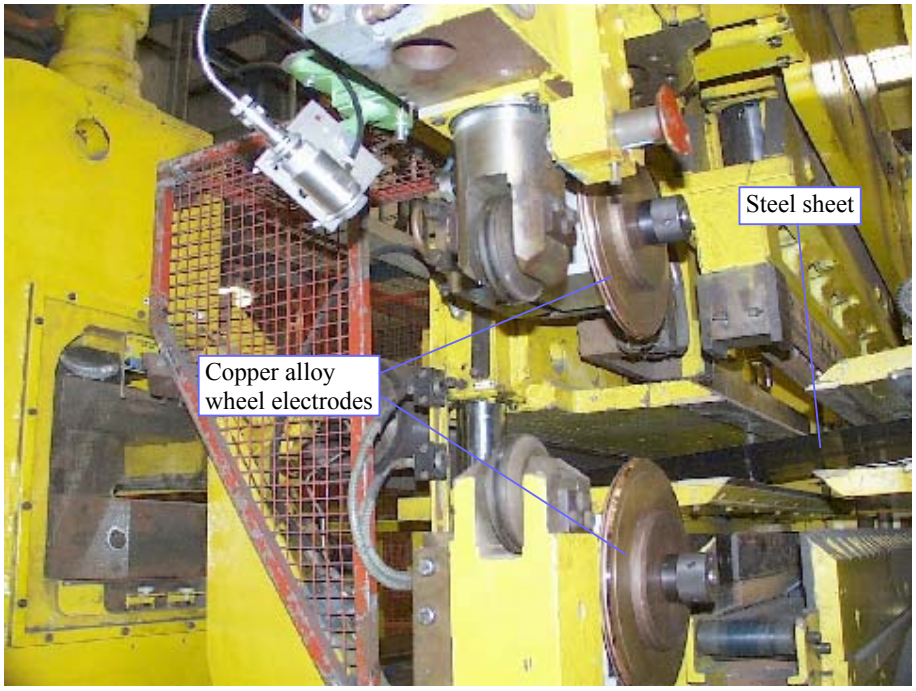

Figure 30: BHP Tin Mill System

Basically, this is a typical pattern classification problem. According to a metallographic report provided by the client, weld quality is classified into one of three categories, *good*, *bad* and *suspect*. During welding, two parameters, namely *voltage* and *current*, are recorded. Thus a preliminary investigation was undertaken to find an efficient technique to construct a relationship between the two main process parameters and weld quality.

After some preliminary work however it became clear that the amount of original classified data was insufficient. In the best case, a single dataset containing 20,000 data points had only 12 classified points; the ratio of classified data to total data was less than 1:1500. Generally artificial intelligence techniques (Neural Networks and Decision Trees) are subjected to some training processes before they are applied. During this pre-processing, large amounts of classified data are required to construct the hyperspace of an investigated environment. Obviously, the low rate of training data available did not lend itself to further analysis.

Furthermore, the other impediment was the realization that the plant operators did not have the ability to alter the system feedback loop in any case. In other words, any changes to voltage and/or current indicated by an Artificial Intelligence classifier (or other techniques) could not be incorporated online.

For these reasons, it was decided to redirect and focus attention to the Gas Metal Arc Welding project, an environment where the operator has more control over system inputs.

APPENDIX 2: PSD Results of Voltage, Power and Resistance Waveforms (Standoff = 10, 15, 20 mm)

A. PSD Results of Voltage Waveforms

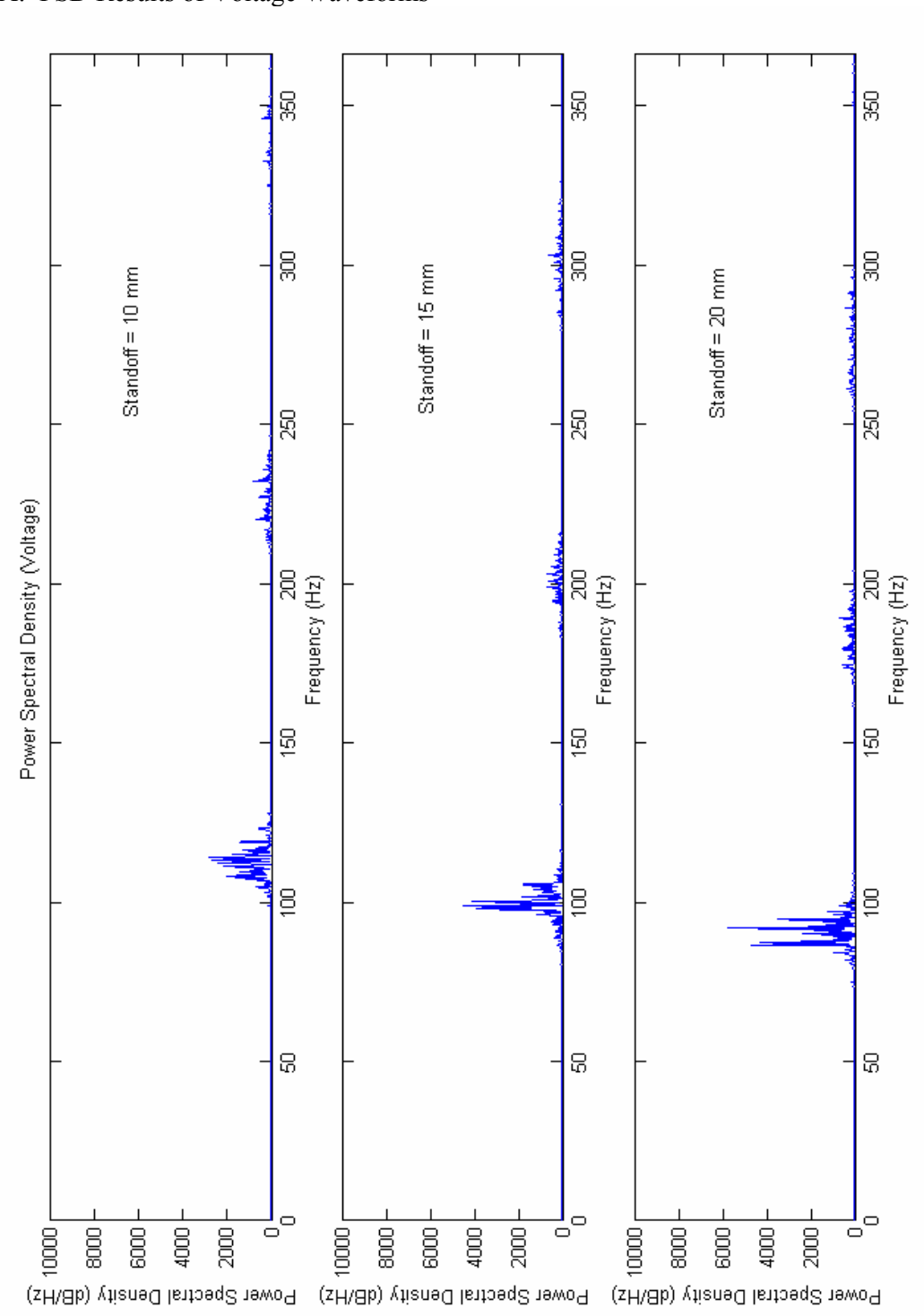

B. PSD Results of Power Waveforms

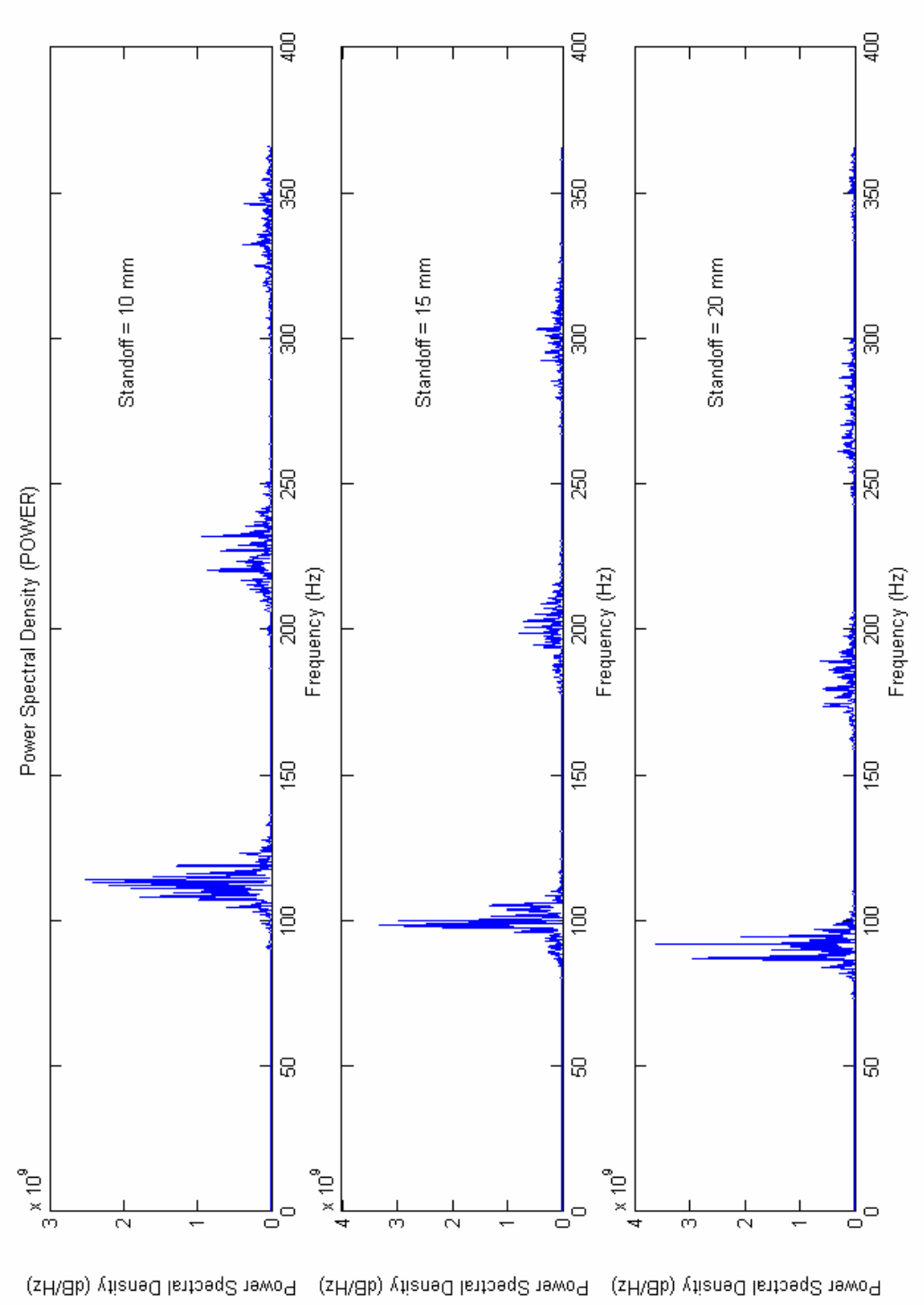

C. PSD Results of Resistance Waveforms

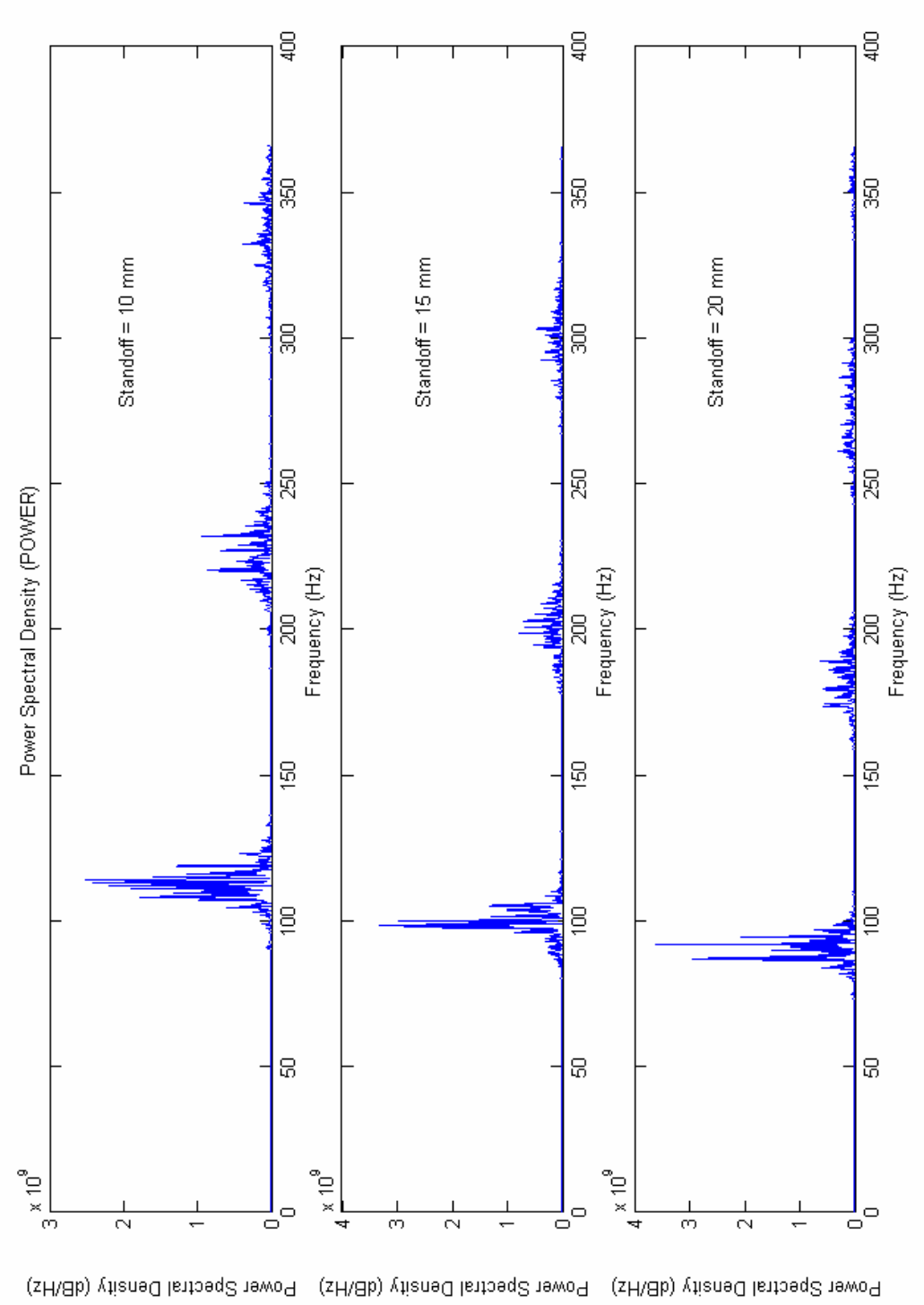

APPENDIX 3: PSD Results of Voltage, Power and Resistance Waveforms (Standoff = 10, 13, 15, 18, 20 mm)

A. PSD Results of Voltage Waveforms

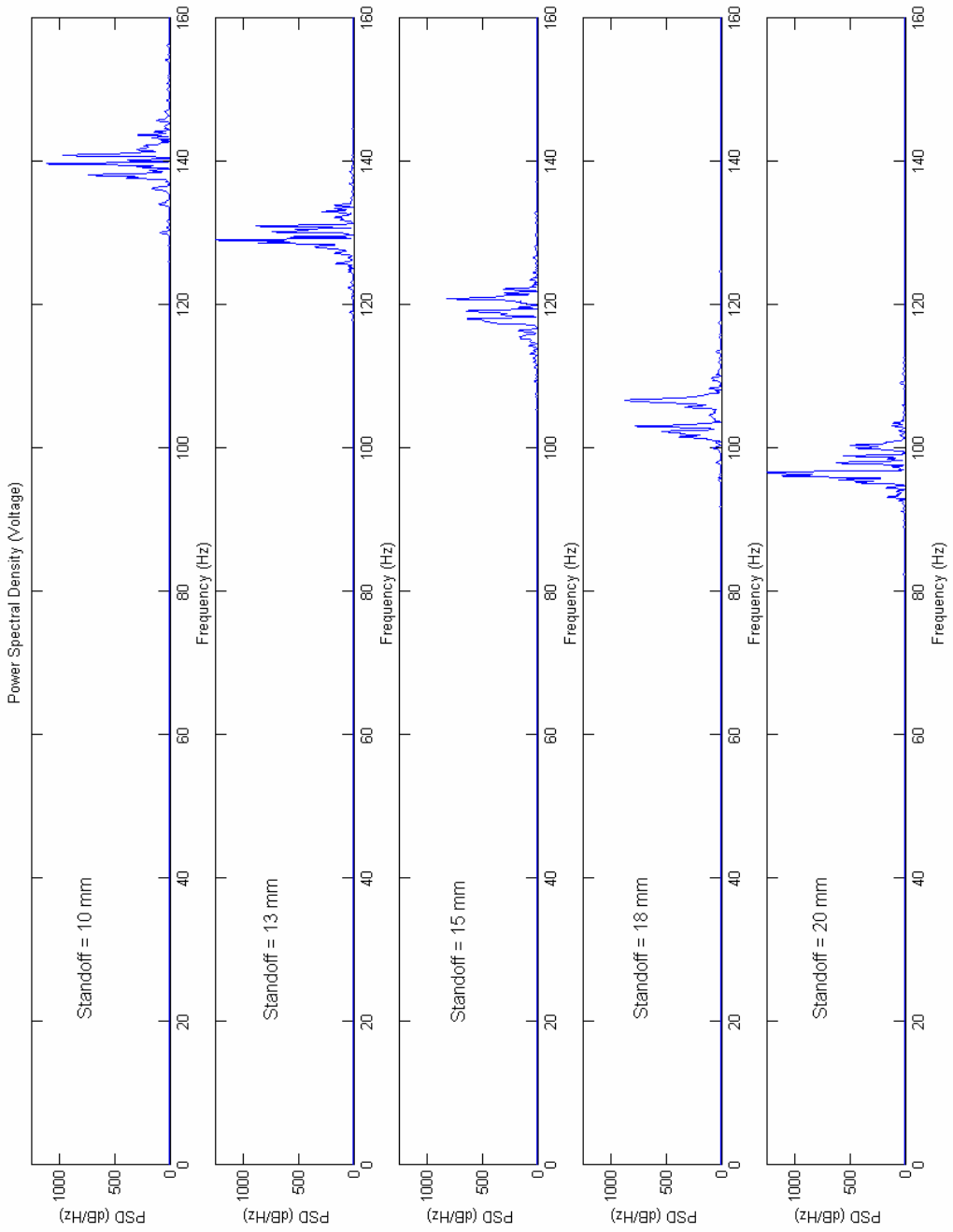

B. PSD Results of Power Waveforms

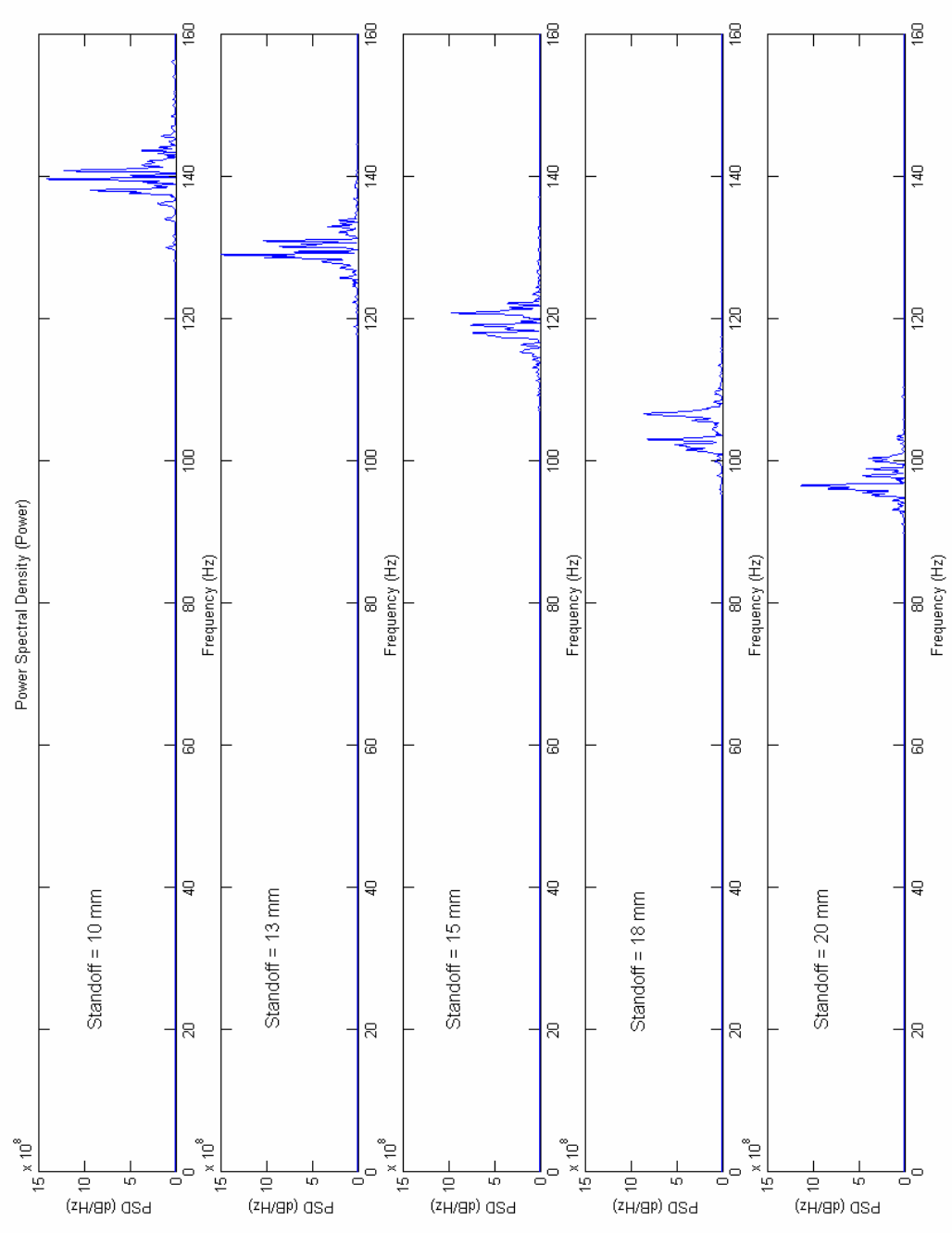

C. PSD Results of Resistance Waveforms

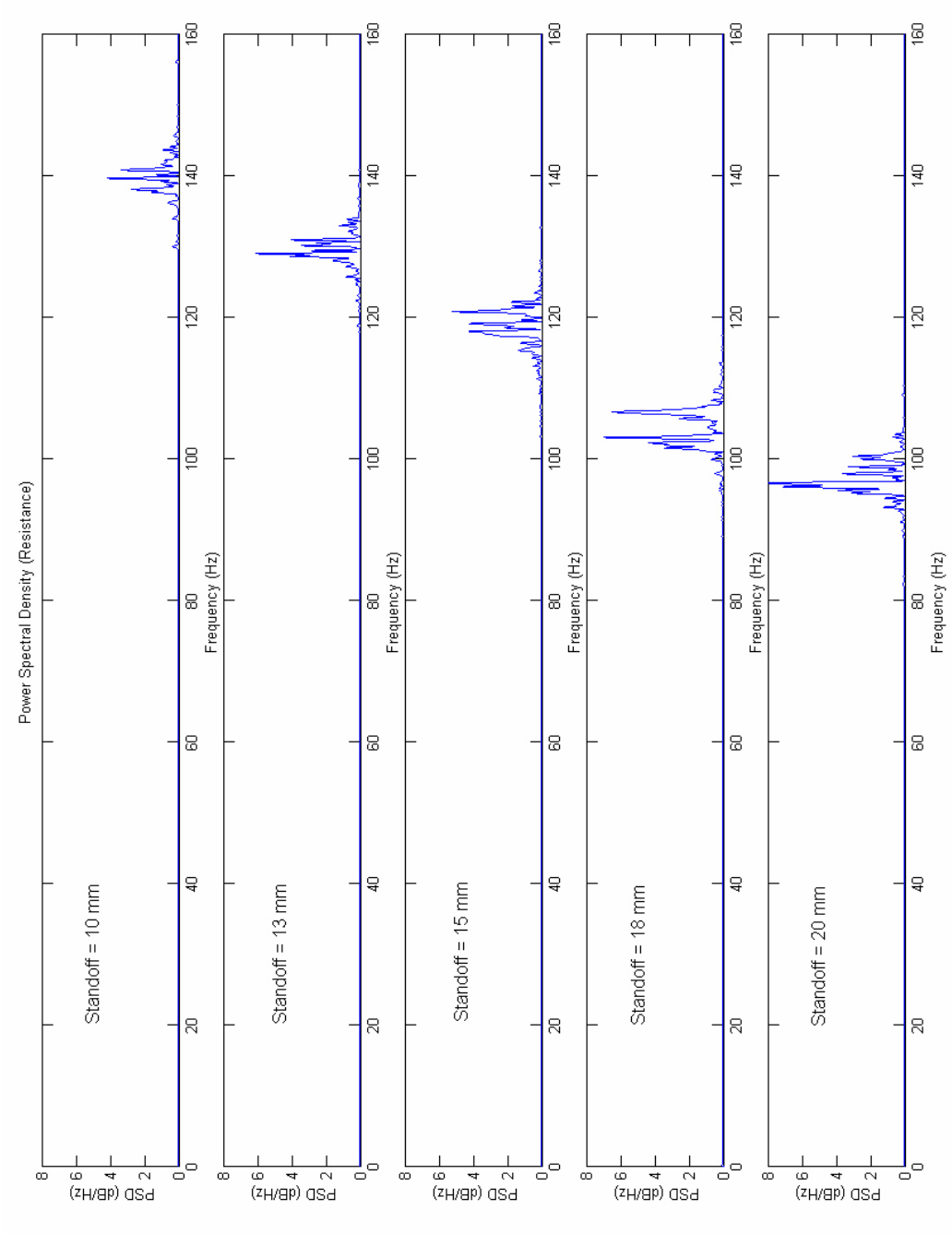

APPENDIX 4: MATLAB Source Codes

A. Trial1.m

```
% This program was designed to analyze welding trials without torch
% oscillation, which were set up on flat plates.
% Three values of CTWD were selected: 10 mm, 15 mm and 20 mm.
%
% Title: Fusion Defect Detection in Pulsed Gas Metal Arc Welding
% Hao SHEN, August 2002.
% Copyright 2002-2003 The University of Wollongong.
%

% environment setting
clear *;
clg;
name = '06Aug*';
ext = 'wgd';

% Read transient data from origianl .wgd file.
for i = 1:3,
    name(6) = '0' + i;
    nameWgd = strcat(name, '.', ext);
    fidin = fopen(nameWgd);
    [temp, count] = fread(fidin,2,'double');
    [VOLTAGE(:,i), vcount] = fread(fidin, temp(2), 'double');
    [CURRENT(:,i), vcount] = fread(fidin, temp(2), 'double');
    [SPEED(:,i), vcount] = fread(fidin, temp(2), 'double');
    fclose(fidin);
end

sampleRate = temp(1);
numPoints = temp(2);
warning off;

fprintf('SampleRate       : %d\n', sampleRate);
fprintf('Number of points : %d\n\n', numPoints);

% Generate power and resistance transient signals.
POWER = VOLTAGE.*CURRENT;
RESIS = VOLTAGE./CURRENT;

% Calculate mean values of current, volatage, power and resistance
% signals, and plot them vs. time.
CTWD = [10 15 20];
mean_V =  mean(VOLTAGE);
mean_I =  mean(CURRENT);
mean_P =  mean(POWER);
mean_R =  mean(RESIS);
fprintf('CTWD            (mm)  : %d\t\t\t%d\t\t\t%d\n', CTWD(1),
CTWD(2), CTWD(3));
fprintf('Voltage mean    (V)   : %6.4f\t\t%6.4f\t\t%6.4f\n',
mean_V(1), mean_V(2), mean_V(3));
fprintf('Current mean    (A)   : %6.4f\t%6.4f\t%6.4f\n', mean_I(1),
mean_I(2), mean_I(3));
```

```
fprintf('Power mean      (W)   : %6.4f\t%6.4f\t%6.4f\n', mean_P(1),
mean_P(2), mean_P(3));
fprintf('Resistance mean (Ohm) : %6.4f\t\t%6.4f\t\t%6.4f\n',
mean_R(1), mean_R(2), mean_R(3));

% Calculate the PSD of current signals.
for i = 1:3
    subplot(3,1,i);
    GetFFT(CURRENT(:,i), sampleRate);
    if i == 1
        title('Power Spectral Density (Current)');
    end;
    axis([0 160 0 1.0e+7]);
end;
pause;

% Calculate the PSD of voltage signals.
for i = 1:3
    subplot(3,1,i);
    GetFFT(VOLTAGE(:,i), sampleRate);
    if i == 1
        title('Power Spectral Density (Voltage)');
    end;
    axis([0 160 0 2.0e+4]);
end;
pause;

% Calculate the PSD of power signals.
for i = 1:3
    subplot(3,1,i);
    GetFFT(POWER(:,i), sampleRate);
    if i == 1
        title('Power Spectral Density (Power)');
    end;
    axis([0 160 0 9.0e+9]);
end;
pause;

% Calculate the PSD of resistance signals.
for i = 1:3
    subplot(3,1,i);
    GetFFT(RESIS(:,i), sampleRate);
    if i == 1
        title('Power Spectral Density (Resistance)');
    end;
    axis([0 160 0 70]);
end;
pause;

clear *;
```

B. Trial2.m

```
% This program was designed to analyze welding trials set up on
% bevelled plates without torch oscillation.
% Five values of CTWD were selected: 10 mm, 13 mm, 15 mm, 18 mm, and
% 20 mm.
%
% Title: Fusion Defect Detection in Pulsed Gas Metal Arc Welding
% Hao SHEN, August 2002.
% Copyright 2002-2003 The University of Wollongong.
%

% environment setting
clear *;
clg;
name = '11Sep*';
ext = 'wgd';

% Read transient data from origianl .wgd file.
numPoints = 15000;

for i = 1:5,
    name(6) = '0' + i;
    nameWgd = strcat(name, '.', ext);
    fidin = fopen(nameWgd);
    [temp, count] = fread(fidin,2,'double');
    [TEMP, count] = fread(fidin, temp(2), 'double');
    VOLTAGE(:,i) = TEMP(1:numPoints);
    [TEMP, count] = fread(fidin, temp(2), 'double');
    CURRENT(:,i) = TEMP(1:numPoints);
    [SPEED(:,i), count] = fread(fidin, temp(2), 'double');
    fclose(fidin);
end

sampleRate = temp(1);
warning off;

fprintf('SampleRate       : %d\n', sampleRate);
fprintf('Number of points : %d\n\n', numPoints);

% Generate power and resistance transient signals.
POWER = VOLTAGE.*CURRENT;
RESIS = VOLTAGE./CURRENT;

% Calculate mean values of current, volatage, power and resistance
% signals, and plot them vs. CTWD.
CTWD = [10 13 15 18 20];
mean_V =  mean(VOLTAGE);
mean_I =  mean(CURRENT);
mean_P =  mean(POWER);
mean_R =  mean(RESIS);
fprintf('CTWD            (mm)  :
%d\t\t\t%d\t\t\t%d\t\t\t%d\t\t\t%d\n', CTWD(1), CTWD(2), CTWD(3),
CTWD(4), CTWD(5));
fprintf('Voltage mean    (V)   :
%6.4f\t\t%6.4f\t\t%6.4f\t\t%6.4f\t\t%6.4f\n', mean_V(1), mean_V(2),
mean_V(3), mean_V(4), mean_V(5));
```

```
fprintf('Current mean    (A)   :
%6.4f\t%6.4f\t%6.4f\t%6.4f\t%6.4f\n', mean_I(1), mean_I(2),
mean_I(3), mean_I(4), mean_I(5));
fprintf('Power mean      (W)   :
%6.4f\t%6.4f\t%6.4f\t%6.4f\t%6.4f\n', mean_P(1), mean_P(2),
mean_P(3), mean_P(4), mean_P(5));
fprintf('Resistance mean (Ohm) :
%6.4f\t\t%6.4f\t\t%6.4f\t\t%6.4f\t\t%6.4f\n', mean_R(1), mean_R(2),
mean_R(3), mean_R(4), mean_R(5));
% Find a linear polynomial fit to the mean values.
ctwd = CTWD(1):0.01:CTWD(5);
p_V = polyfit(CTWD,mean_V,1);
p_I = polyfit(CTWD,mean_I,1);
p_P = polyfit(CTWD,mean_P,1);
p_R = polyfit(CTWD,mean_R,1);

subplot(221);
plot(CTWD, mean_V, 'o', ctwd, polyval(p_V,ctwd));
xlabel('CTWD (mm)');
ylabel('Voltage mean value (V)');
subplot(222);
plot(CTWD, mean_I, 'o', ctwd, polyval(p_I,ctwd));
xlabel('CTWD (mm)');
ylabel('Current mean value (A)');
subplot(223);
plot(CTWD, mean_P, 'o', ctwd, polyval(p_P,ctwd));
xlabel('CTWD (mm)');
ylabel('Power mean value (kW)');
subplot(224);
plot(CTWD, mean_R, 'o', ctwd, polyval(p_R,ctwd));
xlabel('CTWD (mm)');
ylabel('Resistance mean value (Ohm)');
pause;

% Calculate mean peak amplitude current and plot it in diagram vs.
CTWD.
TEMP = CURRENT - 350;
for i = 1:5
    s(i) = 0;
    count(i) = 0;
    for j = 1:15000
        if TEMP(j,i) > 0
            s(i) = s(i) + TEMP(j,i);
            count(i) = count(i) + 1;
        end
    end
    mean_PI(i) = s(i)/count(i) + 350;
end

clg;
pm_I = polyfit(CTWD,mean_PI,1);
plot(CTWD, mean_PI, 'o', ctwd, polyval(pm_I,ctwd));
title('Relationship between CTWD and Mean Peak Amplitude Current');
xlabel('CTWD (mm)');
ylabel('Mean Peak Amplitude Current (A)');
pause;

% Calculate the PSD of current signals.
```

```
for i = 1:5
    subplot(5,1,i);
    GetFFT(CURRENT(:,i), sampleRate);
    if i == 1
        title('Power Spectral Density (Current)');
    end;
    axis([0 160 0 5.0e+6]);
end;
pause;

% Calculate the PSD of voltage signals.
for i = 1:5
    subplot(5,1,i);
    GetFFT(VOLTAGE(:,i), sampleRate);
    if i == 1
        title('Power Spectral Density (Voltage)');
    end;
    axis([0 160 0 5000]);
end;
pause;

% Calculate the PSD of power signals.
for i = 1:5
    subplot(5,1,i);
    GetFFT(POWER(:,i), sampleRate);
    if i == 1
        title('Power Spectral Density (Power)');
    end;
    axis([0 160 0 5.0e+9]);
end;
pause;

% Calculate the PSD of resistance signals.
for i = 1:5
    subplot(5,1,i);
    GetFFT(RESIS(:,i), sampleRate);
    if i == 1
        title('Power Spectral Density (Resistance)');
    end;
    axis([0 160 0 30]);
end;
pause;

% Design a 10th-order bandpass Butterworth filter with a
% passband from 80 to 180 Hz and plot its impulse response.
n = 5;
Wn = [80 180]/2500;
[b,a] = butter(n,Wn);
[h,w]=freqz(b,a,1024*64);
clg;
plot(w*5000/(2*pi),abs(h));
axis([0 200 0 1.2]);
title('Bandpass Butterworth Filter (Order = 10, Cutoff = [80 180]
HZ)');
xlabel('Frequency (Hz)');
ylabel('Magnitude (dB)');
grid on;
pause;
```

```
grid off;

% Filter current signals using a bandpass Butterworth filter.
time = 60*(1:numPoints)/sampleRate;
for j = 1:5
    % Original signals
    subplot(5,2,2*j-1);
    plot(time,CURRENT(:,j));
    if i == 1
        title('Original Current Signals');
    end;
    xlabel('time (s)');
    ylabel('Current (A)');
    axis([5 15 0 600]);

    % Filtered signals
    subplot(5,2,2*j);
    sf(:,j) = filter(b, a, CURRENT(:,j));
    plot(time,sf(:, j));
    if i == 1
        title('Filtered Current Signals');
    end;
    xlabel('time (s)');
    ylabel('Current (A)');
    axis([5 15 -250 250]);
end;
pause;

% Calculate the PSD of filtered current signals and plot the diagram
% vs. CTWD.
for i = 1:5
    subplot(5,1,i);
    peakfrequ(i) = GetFFT(sf(1:1000,i), sampleRate);
    if i == 1
        title('Frequency content');
    end;
    axis([0 150 0 2.0e+5]);
end;
fprintf('Peak Frequency  (Hz)  :
%6.4f\t%6.4f\t%6.4f\t%6.4f\t%6.4f\n', peakfrequ(1), peakfrequ(2),
peakfrequ(3), peakfrequ(4), peakfrequ(5));
pause;

clg;
p_frequ = polyfit(CTWD,peakfrequ,1);
plot(CTWD, peakfrequ, 'o', ctwd, polyval(p_frequ,ctwd));
title('Relationship between CTWD and Mean Peak Amplitude Current');
xlabel('CTWD (mm)');
ylabel('Peak frequency (Hz)');
pause;

% Plot finer resolution of original current signals.
sp = [28 40 32 30 8];            % start plot point
for i = 1:5
    subplot(5,1,i);
    plot(time(1:250), CURRENT(sp(i):sp(i)+249,i));
    if i == 1
        title('Change of Pulse Frequency');
```

```
    end;
    xlabel('time (s)');
    ylabel('Current (A)');
    axis([0 2.5 0 450]);
end;

clear *;
```

C. Trial3.m

```
% This program was designed to analyze welding trials with torch
% oscillation, which were set up on bevelled plates.
% The torch offset-to-joint centerline was set at three different
% values (0 mm, 2 mm, and 4 mm).
%
% Title: Fusion Defect Detection in Pulsed Gas Metal Arc Welding
% Hao SHEN, August 2002.
% Copyright 2002-2003 The University of Wollongong.
%

% environment setting
clear *;
clg;
name = '29Oct*';
ext = 'wgd';

% Read transient data from origianl .wgd file.
for i = 1:3,
    name(6) = '0' + i;
    nameWgd = strcat(name, '.', ext);
    fidin = fopen(nameWgd);
    [temp, count] = fread(fidin,2,'double');
      [VOLTAGE(:,i), vcount] = fread(fidin, temp(2), 'double');
      [CURRENT(:,i), vcount] = fread(fidin, temp(2), 'double');
      [SPEED(:,i), vcount] = fread(fidin, temp(2), 'double');
    fclose(fidin);
end

sampleRate = temp(1);
numPoints = temp(2);
warning off;

fprintf('SampleRate       : %d\n', sampleRate);
fprintf('Number of points : %d\n\n', numPoints);

% Demonstrate that low frequency contents exist in current signals.
GetFFT(CURRENT(:,1), sampleRate);
title('Power Spectral Density (Current)');
axis([0 160 0 5.0e+6]);
end;
pause;

% Design a 4th-order lowpass Butterworth filter with a
% cutoff of 6 Hz and plot its impulse response.
[b,a] = butter(4,6/(sampleRate/2),'low');
[h,w]=freqz(b,a,1024*64);
plot(w*sampleRate/pi,abs(h));
axis([0 30 0 1.2]);
title('Lowpass Butterworth Filter (Order = 4, Cutoff = 6 HZ)');
xlabel('Frequency (Hz)');
ylabel('Magnitude (dB)');
grid on;
pause;
grid off;
```

```
% Filter current signals using a lowpass Butterworth filter,
% and generate the corresponding PSD results.
time = (1:numPoints)/sampleRate;
for j = 1:3
    % Filter signals
    sf=filter(b,a,CURRENT(:,j));
    subplot(3,2,2*j-1);
    plot(time,sf);
    if j == 1
        title('Filtered Current Waveforms');
    end;
    xlabel('time (s)');
    ylabel('Current (A)');
    axis([1 5 100 140]);

    % Calculate PSD
    subplot(3,2,2*j);
    pf(j) = GetFFT(sf(5001:25000), sampleRate);
    if j == 1
        title('Frequency Contents');
    end;
    axis([0 5 0 200000]);
end;

fprintf('Weld Quality        : Good\t\tPoor\t\tPoor\n');
fprintf('Torch Offset   (mm) : 0\t\t\t2\t\t\t4\n');
fprintf('Peak Frequency (Hz) : %6.4f\t%6.4f\t%6.4f\n', pf(1), pf(2),
pf(3));

clear *;
```

D. Trial4.m

```
% This program was designed to analyze a 'diagonal' welding trial
% seting up on bevelled plate with torch oscillation.
% The torch traveled from the edge of the bevel to the centre of the
% groove during welding,
% the offset value changing from 2 mm to 0 mm.
%
% Title: Fusion Defect Detection in Pulsed Gas Metal Arc Welding
% Hao SHEN, August 2002.
% Copyright 2002-2003 The University of Wollongong.
%

% environment setting
clear *;
clg;
sampleRate = 2500;
load 18Dec0.mat;
numPoints = length(CURRENT);

fprintf('SampleRate       : %d\n', sampleRate);
fprintf('Number of points : %d\n\n', numPoints);

% Construct a 4th-order lowpass Butterworth filter with a
% cutoff of 6 Hz and plot its impulse response.
[b,a] = butter(5,10/(sampleRate/2),'low');
[h,w]=freqz(b,a,1024*64);

% Split the given signal into three equal-lenght windows,
% filter the windowed signals using a lowpass Butterworth filter,
% and generate the corresponding PSD results.
time = (1:numPoints)/sampleRate;
sf=filter(b,a,CURRENT);
subplot(2,1,1);
plot(time(1:20001),sf(3450:numPoints));
axis([0 8 80 130]);
title('Time Waveform Using Lowpass Butterworth Filter With Order 4');
xlabel('Time (s) -- cutoff = 6 Hz');
ylabel('Current (A)');
hold on;
pause;

sample = reshape(sf(3450:numPoints), 6667, 3);
for i = 1:3
    subplot(3,3,6+i);
    pf(i) = GetFFT(sample(:,i), sampleRate);
    GetFFTPeak(sample(:,i), sampleRate);
    axis([0 10 0 2.0e+4]);
end;
hold off;

fprintf('Torch Offset (mm)  : 2\t\t\t=====>\t\t0\n');
fprintf('Peak Frequency (Hz): %6.4f\t\t%6.4f\t\t%6.4f\n', pf(1),
pf(2), pf(3));

clear *;
```

E. GetFFT.m

```
% GetFFT calculates the Power Spectral Density (PSD) of a given
% signal using fixed n-point FFT.
%
% Description
%   GetFFT(SAMPLE, sampleRate) takes these arguments,
%       SAMPLE      - a given signal ready to analyze.
%         sampleRate  - sample rate.
%   plots a PSD result, and returns peak frequency pf.
%
% Hao SHEN, August 2002.
% Copyright 2002-2003 The University of Wollongong.
%

function pf = GetFFT(SAMPLE, sampleRate)

numPoints = length(SAMPLE);
n = 1024*32;
frequency = sampleRate*(0:n-1)/n;

TEMP_DAT = SAMPLE - mean(SAMPLE);
TEMP_FFT = fft(TEMP_DAT,n);
TEMP_PSD = TEMP_FFT.*conj(TEMP_FFT)/n;

plot(frequency, TEMP_PSD);
xlabel('Frequency (Hz)');
ylabel('PSD (dB/Hz)');

tempf = TEMP_PSD(1:(n/2));
pf = frequency(find(tempf==max(tempf)));
```

APPENDIX 5: Conference Paper Published

This paper was published on 2nd Int. Conf. on Recent Developments and Future Trends in Welding Technology, Cranfield University, UK, 3rd-5th Sept., 2003.

Through arc adaptive control of GMAW: Requirements for high productivity girth welding of pipe

P. Di Pietro*, J. Norrish*, H. Shen, J. Fulcher****

* Faculty of Engineering, University of Wollongong NSW 2522 Australia
** Faculty of Informatics, University of Wollongong NSW 2522 Australia

Abstract The feasibility of high productivity girth welding of pipelines has previously been demonstrated. Manual adjustment of torch height and seam tracking is not however viable at the high travel speeds used. Fortunately, through arc sensing can be used to monitor and record arc voltage and current. Methodologies developed using these signals are presented to compensate for pipe ovality in-process and to maintain torch tracking whilst weaving. The successful up-take of automated girth welding is dependent on the successful implementation of these control strategies as these important process variables have been identified as being critical for proper weld bead deposition.

Keywords Seam tracking, torch height control, girth welding, pipeline construction

Introduction

Mechanised gas metal arc welding (GMAW) has been adopted widely throughout the world for the field welding of girth joints in transmission pipelines. Most of the common systems use the 'bug on band' type of drive mechanism but rely on an operator to manually adjust torch height and seam tracking whilst the bug rotates around the pipe. Recent developments [1] have led to significant increases in welding speed and a move to automated rather than mechanized systems. While manual adjustment is feasible at linear travel speeds of 300 to 400 mm/min, it is not possible at speeds exceeding 1 m/min. Although every attempt is made to accurately prepare the joint faces; variations in joint fit up, torch offset and pipe ovality are commonplace. In order to effectively utilize the productivity benefits of these higher travel speeds, some form of automatic torch height adjustment and seam tracking becomes necessary.

There are many options available for adaptive control of torch position [2, 3]; these may be classified broadly as those that utilize external sensors and those that use 'through arc' techniques. External sensor systems incorporating laser line scan devices have been found to be effective and although they can be fairly compact, there are still concerns about their overall robustness in a field welding situation. Through arc techniques utilize transient electrical signals from the process to determine torch position. Such systems are inherently more robust but often require sophisticated signal processing to achieve reliable results.

The paper describes two through arc techniques that have been applied to controlled dip transfer root runs and pulsed GMAW fill passes with encouraging results.

Root runs

Torch height regulation

Although it is common to use internal root runs for larger diameter pipe in many instances, in smaller diameter pipe it is desirable to complete the root run externally. Extensive studies in Australia [4] have shown that un-backed root runs can be made satisfactorily using controlled dip transfer. The controlled dip transfer process was originally developed by Boughton et al. [5, 6] at The Welding Institute (TWI) in the UK and is now available in various forms from several manufacturers. The process has been found to be more tolerant than conventional dip transfer in single sided pipe root configurations and gives much more stable operation. This transfer mode is characterized by low heat inputs making it suitable for positional work such as in girth welding of pipe. A useful feature of the process is that when the short circuit occurs (ie. arc extinguishes), the contact tip to workpiece distance (CTWD) represents the contact tip distance from the weld pool as the arc length is zero. This assumes that the contact point within the contact tip is constant. In the case of steel wires, the resistance of the wire in this region is significant and gives a good indication of the wire extension length. According to Ohm's law, in its simplest form:

$$R = \frac{E}{I} \qquad (1)$$

where R is in ohms, E is in volts and I is in amperes.

There are potential problems in calculating the exact resistance of the wire extension due to the variable effect of resistive heating during the short circuit, but these errors are largely avoided in the proposed approach by careful signal processing, the use of consistent controlled short circuit current and ‘self calibration’ of the system on commencement of welding.

Girth welding test bed

A test bed was developed in earlier work and the details of the design are reported elsewhere [7]. The objective of this original work was to evaluate various options for mechanised girth welding of land based pipelines in Australia, specifically the feasibility of welding higher strength (X80), small diameter, thin wall pipe using the GMAW process. Essentially it consists of a fixed ring gear, split clam-shell design that locates directly on the pipe. A carriage is mounted on the track with circumferential, transverse and radial (x, y, z) axes being stepper motor driven. Figure 1 shows a photograph of the system.

Design strategy for automatic torch height control

A data acquisition system was developed that allowed high-speed (5kHz) capture of voltage and current traces. Using equation (1), resistance values were then determined. As a consequence of Ohm's law, the wire extension length is fundamentally assumed to be directly proportional to resistance. However, this condition only holds true during the short-circuiting stage when the wire dips into the weld pool and the arc length is assumed to be negligible.

Figure 2 outlines the control strategy developed. Shortly after initiation of the arc, the process stabilises and a short-circuiting resistance is calculated. It is assumed to represent the pre-determined CTWD, having been correctly set on commencement. As welding proceeds, updated resistance values are determined and continuously monitored against the ideal, initial resistance. If it exceeds a preset percentage deviation from the reference value, the torch height is adjusted. An increase in resistance indicates the torch is further from the pipe joint. The control system then commands the stepper motor controller to drive the torch down until

the process is brought back within acceptable control limits. By analogy, if the resistance is less than the target value then the torch will be directed away from the pipe.

There were several ways in which the reference set-point resistance value can be determined. Initially, minimum resistance values were obtained for consecutive short-circuiting cycles and then averaged. For the welding procedure tested, a short-circuit condition was identified by a fall in voltage below 5V and a subsequent current rise above 50A. This ensures that at this point in time, the process is well within the short-circuiting cycle. The end of the cycle is identified by a rise in voltage above 5V. Another method investigated for determining the target resistance value was to calculate the median resistance within a complete short-circuiting cycle and then averaging over consecutive cycles. However, ultimately the most stable method established was simply to average all short-circuiting resistance values obtained.

In order to develop model flexibility using different welding procedures, it was not assumed that a short-circuit cycle would always be given by the condition of voltage below 5V and subsequent current rise above 50A. The final strategy implemented therefore determines a moving-average of all resistance values in a sample period and then halves the result obtained. The half-average level is lower than the minimum resistances not in short-circuiting mode but greater than the short-circuiting resistances. This is due to the observation that the dip in resistance during short-circuiting is far greater than 50% of all averaged resistances. Resistances falling below the half-mean level are then simply averaged to give the target short-circuiting resistance set-point.

From earlier welding trials it became apparent that torch height should not be continuously controlled each time a resistance value is determined. Even if a constant CTWD condition exists (and regardless of high process stability), no two short-circuiting resistances are identical due to inherent instabilities in the welding process and surface conditions. Such a control strategy would be conducive to poor weld bead quality due to continuous torch movement. Pipe ovality is not a sudden shock process event and thus a step-input control strategy is not appropriate. A threshold adaptive system was therefore developed to provide softer, more gradual control (refer to figure 3).

The upper and lower target thresholds simply represent the bounds that can reasonably be expected from short-circuiting resistance calculations about a central reference value. Numerous welding trials were conducted in order to establish these and the control limits. Again, in order to maintain model flexibility, constant values were not defined as these would require tuning or calibration with any process change. Instead these were calculated as percentile values. Torch height control occurs when the calculated resistance goes above or below the control limits and motion is commanded until the value returns within the bounds of the upper and lower target thresholds.

Implemented control system

Figure 4 shows the final graphical user interface developed for the control system. The user interface (apart from allowing the operator to enter both root pass and fill pass details in order to perform pipeline welding), displays the voltage, current and resistance traces. In order to display data in real-time without adversely affecting the control strategy, a chart buffering system was developed and incorporated into the code. Essentially a subset of data is acquired providing a reasonable snapshot of signal transience although high-speed phenomena is not observable. The display in the lower right-hand corner provides the operator with on-line visualisation of the torch height control. The triangular pointer represents the welding torch, whilst the circle represents the pipe cross-section. A line depicts the CTWD distance as the torch traverses about the pipe circumference. In this particular instance, the display shows the CTWD estimation when welding over a deliberately deposited tack weld to represent severe ovality. The data is also recorded to disc for future evaluation if required.

The approach has proved very acceptable for controlled short-circuiting transfer and has recently been tested at travel speeds over 1 m/min. However, since fill passes are commonly deposited using the pulsed metal transfer mode, the strategy is unlikely to be effective for other than the root pass. In order to overcome this difficulty, pipe ovality data recorded during the initial run can be passed to subsequent weld runs as a path correction algorithm.

The root run is however conducted as a stringer bead (without weaving) and whilst the approach is suitable for torch height control it does not provide any information concerning the lateral position of the torch for seam tracking. This could be addressed using high speed weaving techniques such as those recently reported by Kodama et al. [8] or by employing a variation of the rotating arc technique [9].

Fill Passes

Seam tracking

An open arc, pulsed transfer approach, known as the 'Switch Back' welding technique [10] has recently been used for depositing un-backed root beads whilst weaving simultaneously both across and along the joint seam. However pulsed transfer GMAW is more commonly used for fill passes rather than root runs for the positional welding of pipe. The welding torch is simply weaved across the joint and variations in electrical signals are used to infer torch position for seam tracking control. It has also been shown that the most prominent defect of concern in pipeline girth welds, lack of sidewall fusion (LOF), is commonly associated with torch misalignment. The current work sets out to establish a means of monitoring the torch lateral position during weaving as an early indicator of potential LOF and its suitability for real-time, high speed seam tracking control.

Design strategy for automatic seam tracking

Figure 5 shows the effect of torch offset whilst weaving across a bevelled plate. It is clear that torch offset produces distinct CTWD patterns and it was proposed that these waveforms will be consequently reflected in the through arc signals captured. When the torch remains central to the joint, the resulting CTWD pattern is symmetrical about the seam. However a slight offset results in a more complex waveform that is not symmetrical about the seam and has a smaller, minimum CTWD level than the no offset condition. This is because the torch moves closer to one of the bevelled faces than before. In the extreme case, where all the offset is to one side of the joint, the pattern actually returns to being symmetrical about the seam but the minimum CTWD level is even smaller than in the intermediate case.

The CTWD waveform patterns illustrated in figure 5 show that both amplitude and frequency are affected by changes in torch offset. Because the torch weave frequency is known (set at approximately 1.5 Hz in the experiments), signal processing was carried out on the current waveforms to see if its frequency was reflected in the transient signals. A Butterworth low pass filter was consequently applied (4^{th} order, 6 Hz cutoff frequency) and figure 6 shows the filtered current waveforms obtained at various offsets and their respective spectral contents.

Based on the power spectral densities (PSD's), it can be observed that a peak frequency of 1.5259 Hz was obtained when no torch offset was applied (ie. corrseponding to the torch weave frequency). For both the 2 and 4 mm offset trials, the dominant frequency reduced to 0.7629 Hz, half of the torch weave frequency. This is in agreement with the CTWD frequency patterns proposed in figure 5 and can be used as a simple classification rule for LOF or seam tracking control (ie. when torch offset occurs, the dominant frequency of the current waveform is half that of the torch weave frequency). This was validated at other torch oscillation frequencies and offsets.

Torch height regulation

As mentioned above, not only is CTWD pattern frequency affected by changes in torch offset but so too are amplitude levels. Welding trials were conducted on bevelled plates at various torch heights without weaving. Figure 7 plots the mean values of various process parameters for changing CTWD's, with all relationships identified as linear. The greatest scatter in results was found to exist for mean voltage. This is thought to have arisen from the fact that the power supply used for the experiments was a current-based system, providing greater current signal stability as evident in figure 7 for current means.

Like resistance values, power levels are also a calculated quantity and can be determined from the following equation:

$$P = I.E \qquad (2)$$

where P is in watts, E is in volts and I is in amperes.

A similar trend was found by simply extracting the peak amplitude mean from the original current traces. Again, an inverse, linearly proportional relationship exists (refer to figure 8). This methodology can also be used as a possible torch height control strategy.

According to the welding procedure and power supply settings used, the pulsed metal transfer frequency was established to be approximately 120 Hz. Using Fast Fourier Transform (FFT) analysis, a similar trend was also found in the spectral content of the process signals as in the time-domain. A Butterworth band pass filter was applied to the original signals (10^{th} order, 80 Hz / 180 Hz cutoff frequency). Figure 9 shows frequency-domain plots of filtered current signals showing distinct peak frequencies. It is clear that as CTWD decreases, the peak frequency identified increases. Figure 10 confirms that this relationship is indeed linear.

Commonly, the pulse frequency of a power supply is considered constant for a given mean current. However the current traces indicate that the pulse rate indeed changes according to torch height. This finding was confirmed by the manufacturer of the equipment (Fronius International GmbH) as a means of accommodating changes in burn off. Closer examination of the current waveform traces shows the effect of this control strategy when CTWD changes occur (refer to figure 11). It is important to note that the frequency and amplitude changes in the pulsed current waveform are power source design features. These characteristics result from the ‘arc length control’ (ALC) methodology implemented by the power source designer. Several options exist [2], but once the ALC strategy is known, it may be incorporated into a control system similar to that described above.

Therefore, it can be seen that several (linear) torch height control methodologies have been established, both in the time and frequency domain for pulsed GMAW fill passes. These provide alternatives to the pipe ovality 'memory' feature developed for controlled short-circuiting root runs, where any out of roundness detected during the initial run is passed to subsequent filler passes as an ovality correction algorithm. Further work is currently underway examining which of the proposed methodologies would best suit real-time, high-speed implementation. Although FFT's can be performed very efficiently in real-time, due to the simplicity and linearity of the relationship between mean current values and CTWD, it appears that this strategy would be most appropriate for in-process control.

Conclusions

The feasibility of through arc torch height control has been demonstrated for high productivity root pass girth welding of pipelines. The final methodology developed has been found to be robust and immune from the inherently noisy attributes of the GMAW process. Since pipe ovality occurs gradually, a threshold adaptive control system was found to be appropriate as it

provides softer, more gradual control and allows real-time display charting to occur simultaneously. The system has been tested with extremely demanding pipe ovality conditions not expected in practice and has proven acceptable.

Through arc seam tracking and torch height control strategies have also been proposed for pulsed GMAW fill passes. The results show promise as all the through arc signal processing techniques developed are based on simple, fundamental arc physics and show linear relationships to CTWD.

Acknowledgments

The authors wish to acknowledge the contributions of Scott Trenholme, Paul Bergman, Somchai Rayakul and Minh Tieu from the University of Wollongong for the development of the torch height software. Thanks also extend to the CRC for Welded Structures (CRC-WS) and the Australian Pipeline Industry Association for sponsoring some of the work. The CRC-WS was established and is supported under the Australian Government's Cooperative Research Centres Program.

References

[1]. Blackman, S., Walker, P., Michie, K. (2001) High speed tandem GMAW. *1st Int. Conf. on Recent Developments and Future Trends in Welding Technology*, Cranfield University, UK 3-4 September.

[2]. Norrish, J. (1992) *Advanced Welding Processes*. Publ. Institute of Physics, UK (ISBN 0-85274-326-2).

[3]. *Sensors and Control Systems in Arc Welding, Welding Guide Book II* (1991). Technical Commission on Welding Processes, Japan Welding Society.

[4]. Norrish, J., and Di Pietro, P. (2002) Mechanised girth welding options for high strength thin wall pipe. *Int. Conf. on Pipeline Construction Technology*, Wollongong, Australia 4-5 March.

[5]. Boughton, P., and MacGregor, G.J. (1974) Control of short circuiting in MIG welding. *Welding Research International*, Vol. **4** (2) pp. 31-53.

[6]. Norrish, J. (2003) A review of metal transfer classification in arc welding. *IIW document XII-1769-03*, Bucharest, Romania 6-11 July.

[7]. Mills, L., Graham, D., Jager, R., and Norrish, J. (2000) Design and evaluation of a mechanised pipeline girthwelder. *Proc. of WTIA, IIW Asian Pacific International Congress*, paper 8 Melbourne, Australia 29 October - 2 November.

[8]. Kodama, S., Ichiyama, Y., Ikuno, Y., and Baba, N. (2003) A mathematical model of short-circuiting transfer in high speed oscillating MAG process – development of automatic MAG welding machine with arc sensor and its application to field welding of gas pipelines. *IIW document XII-1758-03*, Bucharest, Romania 6-11 July.

[9]. Nomura, H., Sugitani, Y., Kobayashi, Y., and Murayama, M. (1991) Development and application of arc sensor control with high speed rotating arc process. *Sensors and Control Systems in Arc Welding*, Japan Welding Society.

[10]. Oshima, K., Yamamoto, H., Ishihara, T., Kubota, T., Eguchi, K., and Yamane, S. (2003) Adaptive control of back bead in V groove welding without a backing plate. *IIW document XII-1962-03*, Bucharest, Romania 6-11 July.

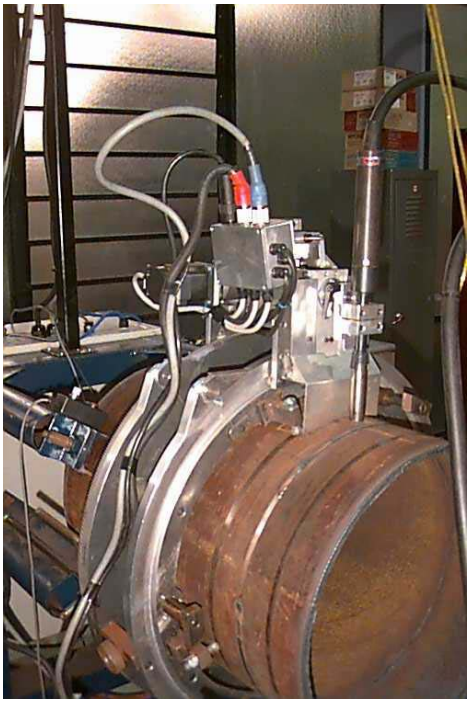

Figure 1 Girth welding test bed.

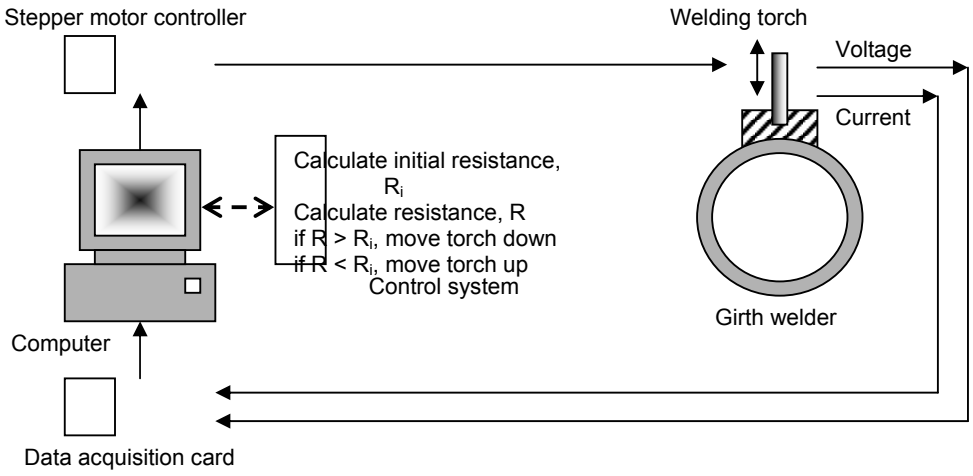

Figure 2 Through-arc sensing and control strategy for root run torch height regulation.

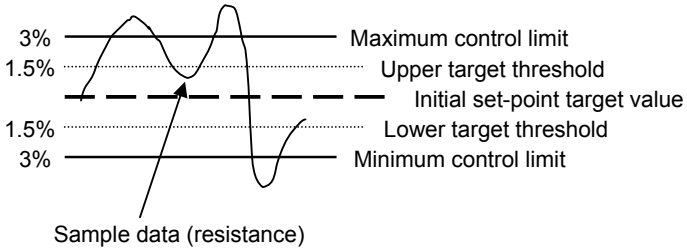

Figure 3 Threshold control system developed.

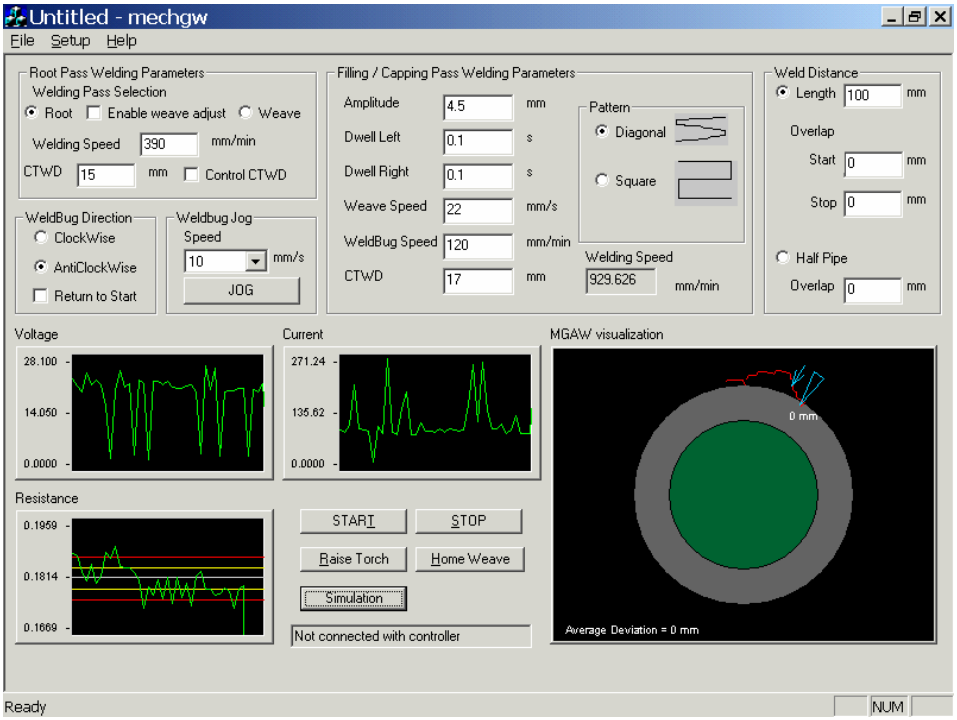

Figure 4 Display screen for operating the girth welding test bed.

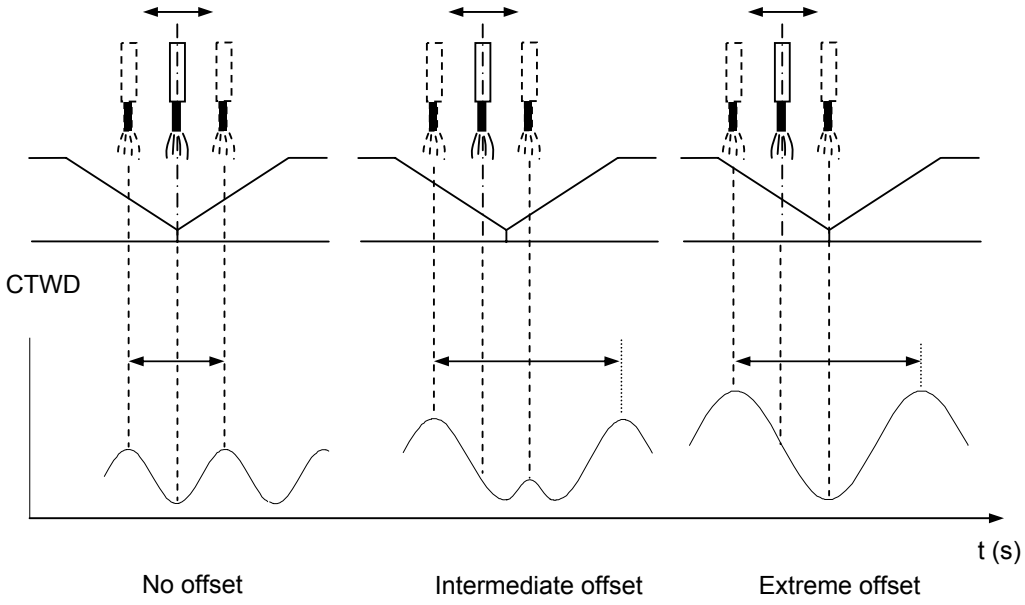

Figure 5 Effect of torch offset on CTWD patterns.

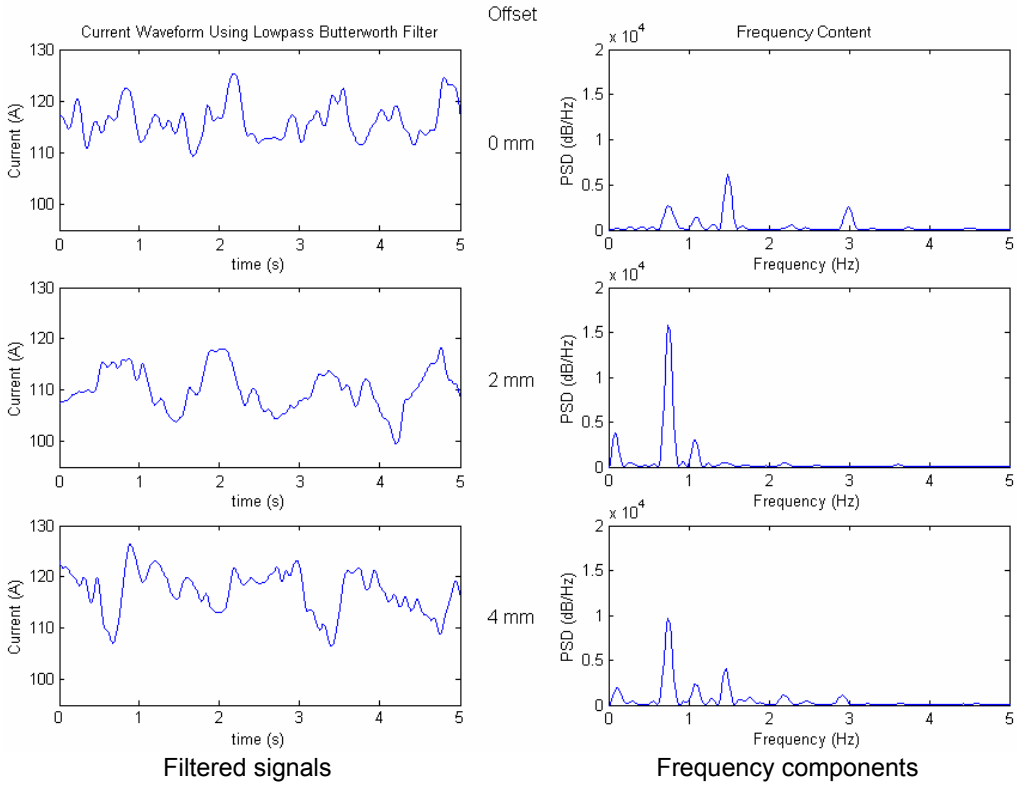

Figure 6 Filtered current waveform traces and corresponding frequency distributions.

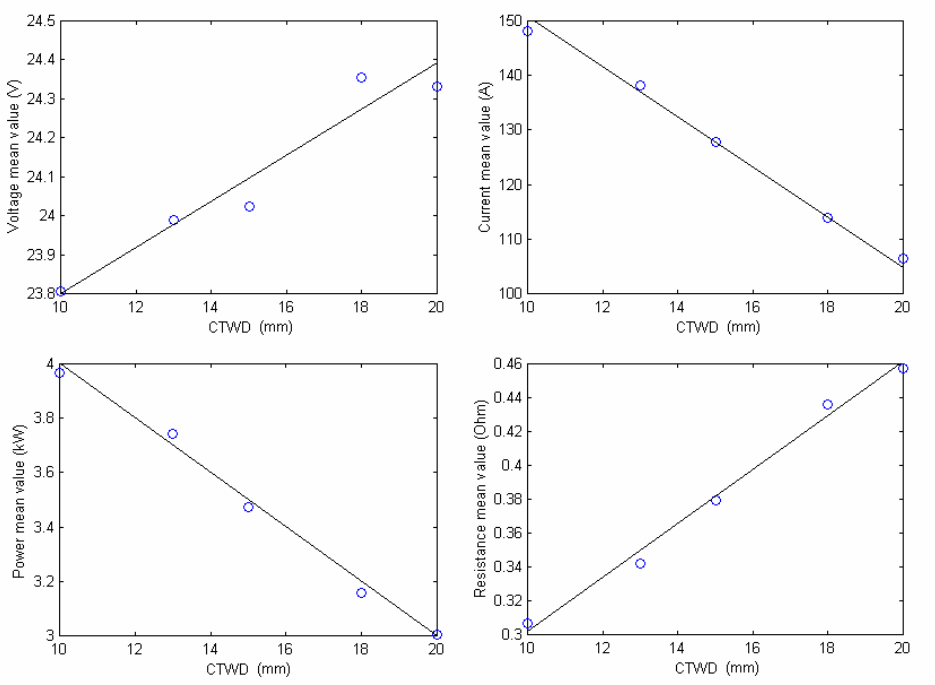

Figure 7 Mean process parameters as a function of changing CTWD.

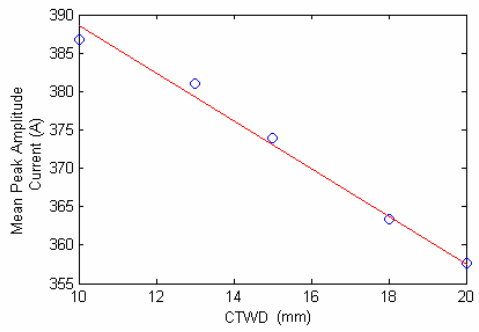

Figure 8 Mean peak amplitude current as a function of changing CTWD.

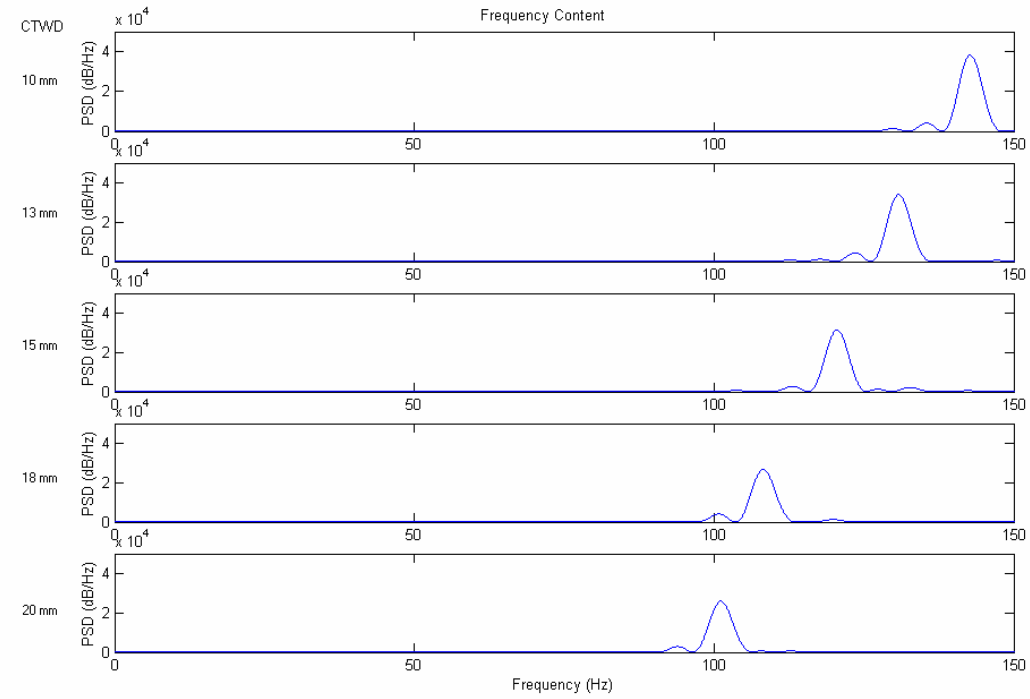

Figure 9 Frequency distributions of current waveforms for changing CTWD.

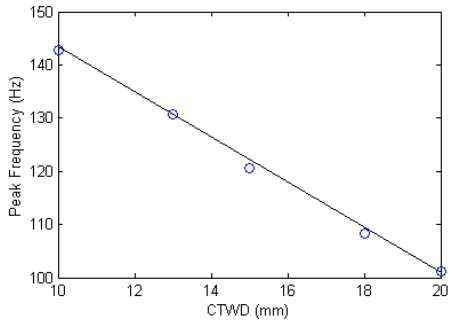

Figure 10 Peak frequency as a function of changing CTWD.

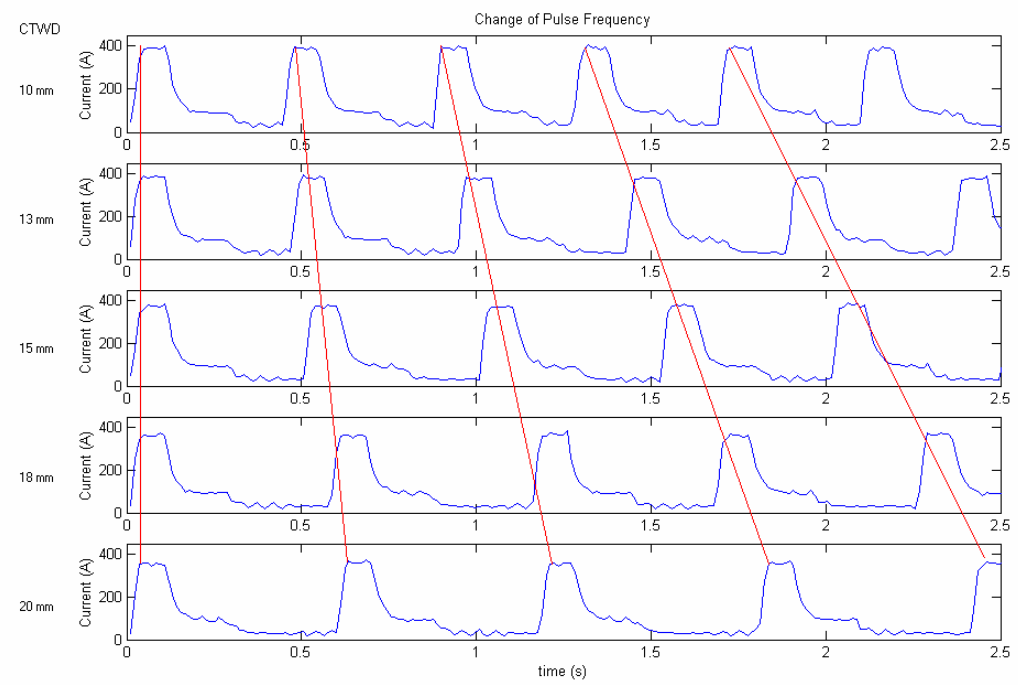

Figure 11 Current waveform traces for various CTWD's indicating the power source ALC strategy implemented.